GPO PRICE $ _____

CFSTI PRICE(S) $ _____

Hard copy (HC) _3 00__

Microfiche (MF) _.65 __

ff 653 July 65

(ACCESSION NUMBER)

(PAGES)

(NASA CR OR TMX OR AD NUMBER)

(THRU)

(CODE)

(CATEGORY)

FACILITY FORM 602

development      components

research      systems

manufacture      instruments

# BARNES ENGINEERING COMPANY

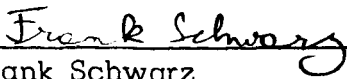## 30 Commerce Road     Stamford, Connecticut

BARNES ENGINEERING COMPANY
30 Commerce Road
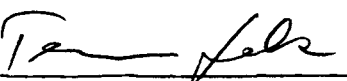Stamford, Connecticut

PART I

FINAL ENGINEERING REPORT

IMMERSED THERMISTOR DETECTOR

OPTIMIZATION PROGRAM

BEC PROJECT 2034

Prepared for

Goddard Space Flight Center
Greenbelt, Maryland

Contract No. NAS-5-10208

PREPARED BY:

*Frank Schwarz*

Frank Schwarz
Head, Advanced Systems Dept.

*Thomas Falk*

Thomas Falk
Asst. Head, Advanced Systems Dept.

Measurements Made By:

Margot B. Brill

APPROVED BY:

*Robert W Astheimer*

R. W. Astheimer
Technical Director
DEFENSE & SPACE DIVISION

DATE:   May 31, 1967

PART I

## TABLE OF CONTENTS

PART I

LIST OF ILLUSTRATIONS

PART I

LIST OF TABLES

## 1. INTRODUCTION

This report is submitted in two parts. Part I describes the effort given to the construction and evaluation of experimental thermistor detectors in connection with the Immersed Detector Optimization Program, together with our conclusions and recommendations. Part II covers the application of controlled cooling techniques to an immersed thermistor detector; the engineering prototype of an optimized immersed thermistor detector, preamplifier, bias supply and cooler package delivered under this contract; and the investigation made to determine the possibilities of using a-c bias. An engineering memorandum on low-noise preamplifiers is included as Appendix A.

To permit easy assessment of the scope of improvements achieved and evaluation of the sensitivity of optimized thermistor detectors for the Nimbus radiometer application, a summary of the over-all results is given in this section.

### 1.1 Summary of Overall Results of Detector Optimization Program

Increased detector sensitivity was achieved ranging from factors of about 2.5 to 4.25, depending on the frequency region of interest. The significant areas in which improvements were made include the following:

1. Use of thin detector flakes whose principal advantage is a decrease in time constant.

2. Use of extremely thin coats of blackening to further decrease time constant. (This measure is effective in the 10 - 12 micron spectral band of interest.)

3. Optimization of operating temperature, both to increase responsivity and to decrease time constant.

4. Use of a new low-noise parametric amplifier to effectively eliminate noise figure degradation produced by the conventional amplifier (principally at the very low frequencies).

5. Operation at higher levels of bias than are normally used with thermistor detectors, primarily to obtain an increase in responsivity.

The development of a technique and equipment for measurement of transducer noise down to extremely low frequencies has, we believe for the

first time, made possible the measurement of thermistor $1/f$ noise at frequencies as low as 0.05 Hz. This has given new insight into the character of the noise in thermistor detectors. The low-noise preamplifier is an essential ingredient in the noise measurement system, since measurements thus made reflect the detector noise to the exclusion of other sources of noise. For typical thermistor impedances, the amplifier may be considered essentially free from low frequency noise.

Study and experimentation with a-c biased detectors showed essentially no improvement in achievable detectivity at any frequency.

An expression has been developed to determine the penalty factor for a detector which is too slow for the intended application, thus permitting better specification of the detector characteristics for an optimum Nimbus scanning radiometer. The performance of the improved detector has been assessed in terms of the ultimate achievable sensitivity for a detector of this basic design, and found to be extremely close to the thermal noise limit in the mid-frequency range. These findings permit us to determine the remaining weaknesses of the detector and areas in which further improvements can be made. Suggestions have already been made for analytical and experimental work to bring about further improvements in detector performance in the low and high frequency regions of the frequency spectrum covered by a Nimbus scanning radiometer.

Table I-1 is a tabulation of the improvement factors obtained for various measures taken. The numbers shown are representative of the average of the detectors measured. This table shows that improvements were achieved ranging from factors of 2.5 to 4.25, depending on the frequency region of the measurements. For instance, detectors of 8 micron thickness have provided us with a S/N improvement factor of 1.2 and a time constant decrease of 1.28 when the normal full course of blackening is applied. The time constant is improved by a factor of 1.5 compared with the detector of standard thickness (16 microns) when only a single coat of APB black is used. Typical time constants measured for thin detectors with one coat of APB range from 0.7 msec. at 25°C to as fast as 0.5 msec. at -25°C when using a bias level of 0.8 $V_{pk}$.

Figure I-1-1 shows typical differences in time constant and spectral response characteristics for detectors of standard thickness as they appear before and after application of three coats of APB black. The time constants for the upper and lower curves are not identical because they are for different detectors. Because the spectral response measurement is not easily accomplished unless the detector is finished and mounted in an enclosed capsule,

these measurements had to be made separately for different detectors. An interesting result shows that a flake of standard thickness does not show greatly increased responsivity at 10 - 12μ when blackened. On the other hand, a thin flake detector has poor responsivity before blackening, probably because of the shorter path length through the material and hence a lower absorptance. To bring the responsivity to the desired level, it appears necessary to apply one thin coat of the blackening agent.

The improvement factors achieved through cooling (possibly space cooling) and through operation at increased levels of bias are seen both from Table I-1 and Figure I-1-2. Figure I-1-2 also shows the detectivity limit for our particular detector construction.

If all the improvements which we have investigated are incorporated, including the use of a high resistance compensator flake, we expect to be thermal-noise limited at frequencies above the 1/f noise region. The thermal noise equivalent power ($NEP_{th}$) for our detector can be expressed as:

$$NEP_{th} = \left(\frac{4KT^2 \Delta F}{Z}\right)^{\frac{1}{2}}$$

where Z is the thermal impedance of the detector, and $\Delta F$ is the bandwidth. For the thin flake detectors, we have measured a thermal impedance of about 800°C/watt.

At an operating temperature of 248°K (-25°C)

$$NEP_{th/cycle} = 5.5 \times 10^{-11} \text{ watt}$$

This figure applies to our 0.2 mm detector. Normalized for a 1 cm detector, this becomes $50 \times 5.5 \times 10^{-11} = 2.75 \times 10^{-9}$ watt and the corresponding maximum $D^* = \frac{1}{NEP} = 3.6 \times 10^8$ cm-cps$^{\frac{1}{2}}$-watt$^{-1}$, shown in Figure I-1-2 as the limit of detectivity for our detector. Since $Z = \frac{\tau_c}{H}$ (where H = heat capacity and $\tau_c$ = detector time constant), the thermal constants can be modified to increase the thermal impedance of the detector and thus achieve a higher $D^*$ limit. But this would result in a degradation in time constant, and the penalty in signal-to-noise ratio at the higher frequency would be very unfavorable.

Since the D* value approaches the detectivity limit in the middle frequency region (40 - 100 HZ), it is evident that further work toward improvement in this region is likely to be fruitless. It is logical, therefore, that future efforts to improve performance of immersed thermistor detectors should be directed toward a reduction in noise which occurs at low frequencies (in the 1/f noise region) and toward continued improvements in the high frequency domain.

TABLE I-1-1  IMPROVEMENTS IN IMMERSED THERMISTOR DETECTOR

| Measure Taken to Obtain Improvement | Time Constant (ms) | Factor by Which Value is Increased | | | | | | | | |
|---|---|---|---|---|---|---|---|---|---|---|
| | | At f = 1 Hz | | | At f = 40 Hz | | | At f = 300 Hz | | |
| | | Signal | Noise | S/N | Signal | Noise | S/N | Signal | Noise | S/N |
| Reference Detector (16μ thick) | 1.5 | 1 | 1 | 1 | 1 | 1 | 1 | 1 | 1 | 1 |
| 1. Thin Det. – Std. Black (8μ thick) | 1.17 | 1.7 | 1.4 | 1.2 | 1.7 | 1.4 | 1.2 | 2.25 | 1.4 | 1.6 |
| 2. Thin Det. – 1 Coat APB | 0.95 | 1.6 | 1.4 | 1.14 | 1.6 | 1.4 | 1.14 | 2.8 | 1.4 | 2 |
| 3. Cooling to –25° and 0.8 $V_{pk}$; Thin Det. – 1 Coat APB | 0.7 | 7.7 | 3.5 | 2.2 | 7.5 | 4.2 | 1.8 | 17.5 | 4.2 | 4.2 |
| 4. Parametric Amplifier | 0.7 | 1.0 | 0.7 | 1.4 | 1.0 | 0.9 | 1.1 | 1.0 | 1.0 | 1.0 |
| 5. Projected Use of High Resistance Compensator | 0.7 | 2.0 | 1.4 | 1.4 | 2.0 | 1.4 | 1.4 | 2.0 | 1.4 | 1.4 |
| Total Improvement Factor Items 3 & 4 | | | | 3.0 | | | 2.0 | | | 4.2 |
| Total Improvement Factor Items 3, 4 & 5 | | | | 4.2 | | | 2.8 | | | 5.9 |
| Expected D* (11μ, f, 1) With all possible improvements (cm-cps$^{\frac{1}{2}}$-watt$^{-1}$) | | | | $0.33 \times 10^8$ | | | $2.8 \times 10^8$ | | | $2 \times 10^8$ |

NOTE:  See Table I-1-2 for improvement factors computed for a wide-band scanning system.

- 5 -

## TABLE 1-1-2

### SUMMARY OF IMPROVEMENTS IN S/N FOR OPERATION IN A BANDWIDTH OF 0.04 – 300 Hz IN THE SPECTRAL BAND 10 – 12μ

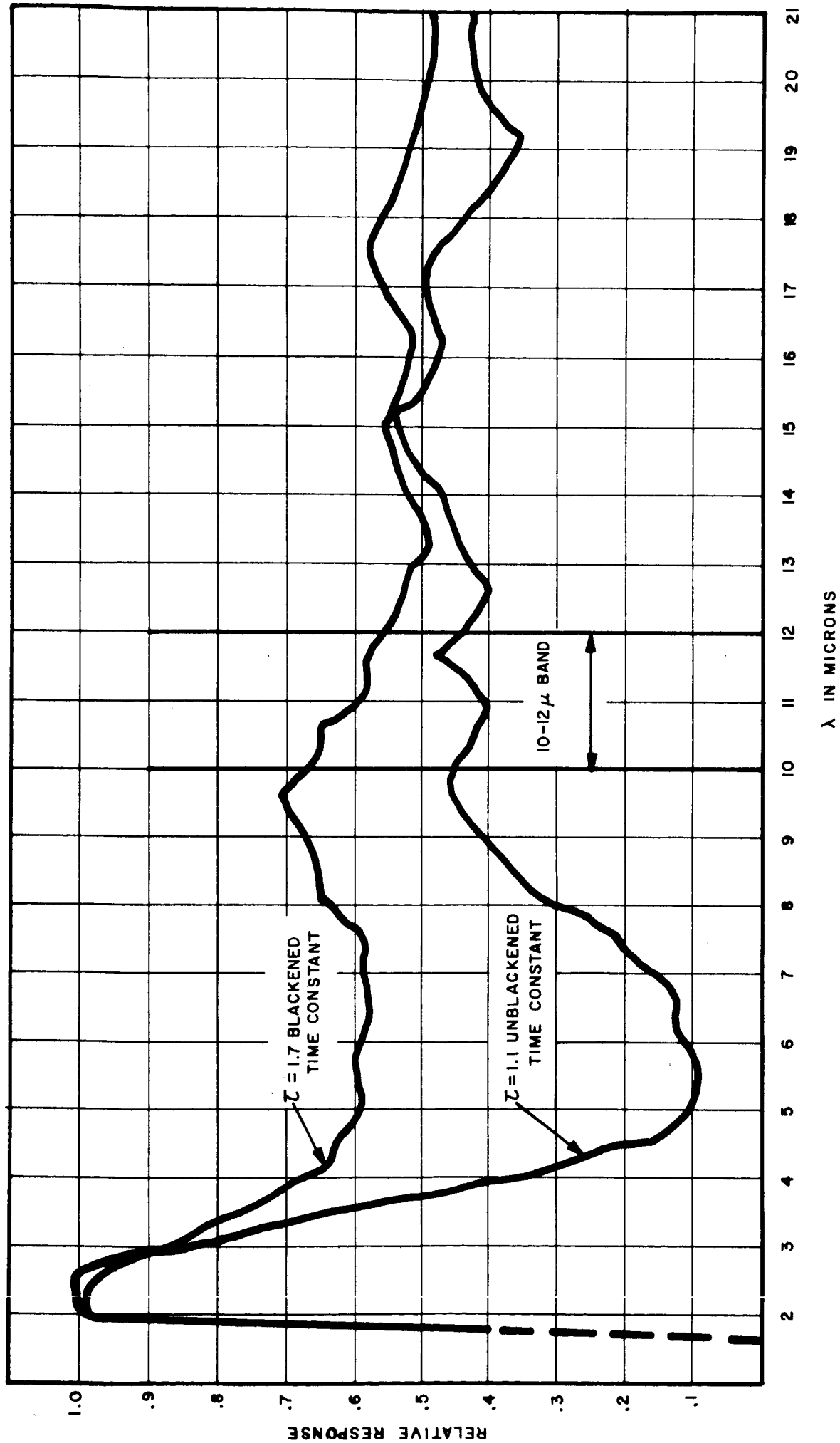| Measurement | Std. Det. 25°C $0.6\,V_{pk}$ | Std. Det. -10°C $0.8\,V_{pk}$ | Thin Flake (Opt. Black) -10°C $0.8\,V_{pk}$ |
|---|---|---|---|
| $D^*$ (10 – 12μ) Wide Band (0.04 – 300) | $1.2 \times 10^8$ | $1.8 \times 10^8$ | $2.1 \times 10^8$ |
| $\tau_c$ (Time Constant) | 1.6 ms | 1.2 ms | 0.8 ms |
| Penalty Factor (See Fig. 4-1) | 5.3 | 3.8 | 2.3 |
| $M_{WB}$ Wide Band Figure of Merit $M_{WB} = \dfrac{D^*}{\text{Penalty F.}}$ | $\dfrac{1.2 \times 10^8}{5.3} = 2.27 \times 10^7$ | $\dfrac{1.8 \times 10^8}{3.8} = 4.7 \times 10^7$ | $\dfrac{2.1 \times 10^8}{2.3} = 9.1 \times 10^7$ |
| Improvement Factor over Standard Detector and Standard Operating Conditions | 1 | 2.07 | 4 |

Figure I-I-I  SPECTRAL RESPONSE, STANDARD THICKNESS THERMISTOR
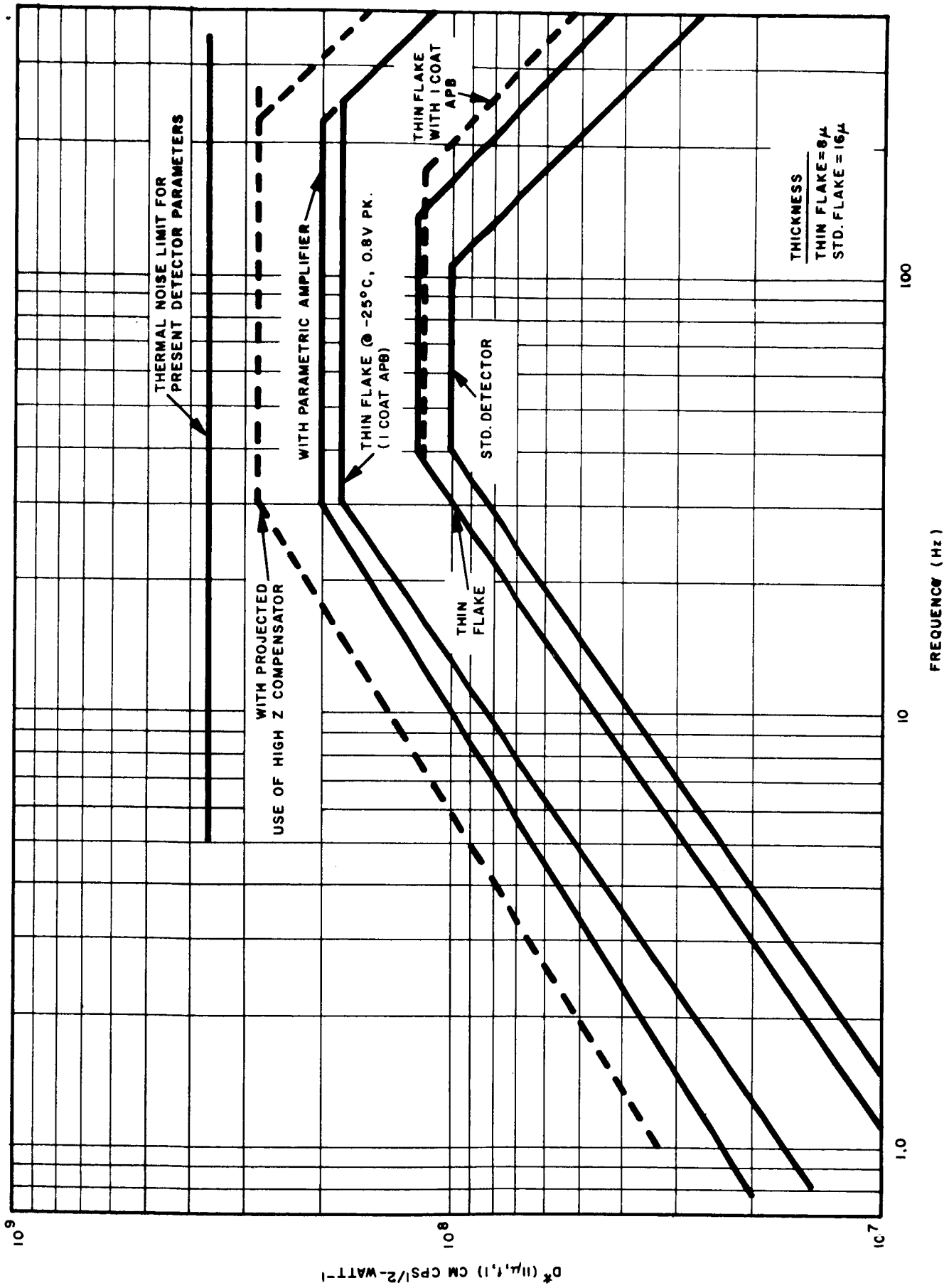
**Figure I-I-2** DETECTIVITY OF IMMERSED THERMISTOR DETECTORS (AVERAGES) AS INFLUENCED BY VARIOUS IMPROVEMENT MEASURES UNDERTAKEN

## 2.2  Measurement Set-Up

Measurements were made on detectors both during the process of detector fabrication and, in more detail, after the detectors had been completely assembled.  The tests during fabrication and after assembly were made with the standard Bolometer Response Analyzer (BRA).

The balance of the tests were made on the Bolometer Test Console (BTC), which had to be drastically modified for this purpose.  This test console, already very versatile, had to be provided with a special rig for cooling the detector to temperatures as low as -40°C, as well as with a special instrument to measure narrow band noise at very low frequencies.  This instrument, known as the Low Frequency Spectrum Analyzer, has been described in detail in the Interim Engineering Report; a photograph of the instrument is shown in Figure I-2-1.

A special filter with a passband of 9.8 - 11.7 microns was procured and installed in the test equipment.  The low-energy throughput of the filter required a rather thorough revamping of the detector measurement equipment to insure a satisfactory signal-to-noise ratio under all conditions of measurement, and thereby provide the desired accuracy and reproducibility of the numerous measurements.

The bulkiness of the detector cooler vacuum enclosure package also necessitated some major changes in the test set.  The blackbody source had to be removed and an entirely new platform had to be constructed to support the detector/cooler package, the special preamplifier, a new variable speed chopper, the filter/aperture plate and blackbody source.  Since the amplifier used was not the one in the test console and the noise measurement equipment and variable speed chopper were likewise changed, about the only instrumentation used in its original form was the bias supply and some of the standard test instruments.  The test set was also used to measure the detector sensitivity in various portions of the infrared spectrum.  A photograph of the test set is shown in Figure I-2-2.

The spectral characteristic of the filter used is shown in Figure I-2-3. To obtain an exact measurement of power on the detector from a blackbody source when this narrow band filter was in use, calculations were made and a curve drawn as shown in Figure I-2-4.  With the known throughput of the optical filter, the blackbody aperture dimensions and the known distance between the detector and the blackbody aperture, the energy received by the detector in the spectral band used was calculated. This parameter, computed in paragraph 2.3, was then used to give the measure of sensitivity of the various detectors tested.

## 2.3  Calculation of Power Received by the Detector

The test set was arranged as shown in Figure I-2-5.

The energy received by the detector from the target source is determined below.

The power on the detector is given by:

$$P_D = \frac{\Delta N_{\Delta\lambda} \, A_d \, A_t \, \epsilon}{d^2}$$

where:

$A_d$ = detector area = $0.02 \times 0.02$ cm = $4 \times 10^{-4}$ cm$^2$

$A_t$ = target aperture area = $1.26$ cm$^2$

$d$ = distance from target to detector = 10 cm

$\epsilon$ = efficiency of optical elements; assume 0.8 transmission due to KRS-5 window.  The optical throughput of the narrow band filter is taken into account along with the spectral transmission of the filter in $\Delta N_{\Delta\lambda}$.  The transmission losses of the detector's germanium blank, for which no correction is made here, are considered to exist in the final germanium immersion lens.

$$\Delta N_{\Delta\lambda} = N_T \frac{1}{F} = \frac{(N_{\lambda s} - N_{c\lambda}) \, \tau_\lambda \Delta\lambda}{N_s - N_c} \text{ , as given in Figure I-2-4, =}$$

radiance of the source in the spectral region of interest which passes through the filter.  This includes the filter transmission.

For the temperature used, 850°C,

$$N_T = 2.8 \text{ watts/cm}^2\text{-ster}$$

and the filter transmission and spectral narrowing results in a filter factor, $F = 62$. (See Figure I-2-4.)

$$\Delta N_{\Delta\lambda} = 0.045 \text{ or, in terms of RMS power, } 0.02$$

$$P_D = \frac{0.02 \times 4 \times 10^{-4} \times 1.26 \times 0.8}{10^2} = 8 \times 10^{-8} \text{ watt}$$

With this information and the measured output signals, a figure of noise equivalent power and detectivity for each detector measured can be obtained. We assume that the power on the detector is $10^{-7}$ watt. From this, knowing the signal-to-noise ratio under given conditions of ambient temperature, bias, etc., we can compute the detectivity. The use of this data is illustrated in the next section.

As an example of one such measurement, we refer to data gathered with detector #5826, a thin flake detector with a time constant of about 1 msec. At 0°C and with 0.8 $V_{pk}$ for that temperature applied to the detector, the measurement indicated a signal output of 380 mV RMS at 100 Hz. The noise was measured as 1.25 mV, at the same frequency, in a $7\frac{1}{2}$ Hz bandwidth ($V_n = 460\mu V$ RMS/cps). The signal-to-noise ratio is thus $\frac{380 \text{ mV RMS}}{460 \text{ }\mu V \text{ RMS}} = 830$. The Noise Equivalent Power is:

$$\text{NEP } (10-11\mu, 100, 1) = \frac{P_D}{S/N} = \frac{10^{-7}}{830} = 1.2 \times 10^{-10} \text{ watt}$$

for a 0.2 x 0.2 mm detector. For a 1 cm$^2$ detector, the area correction is:

$$\sqrt{\frac{1 \text{ cm}^2}{A_d}} = \sqrt{\frac{1}{4 \times 10^{-4}}} = 50$$

The detectivity:

$$D^* = \frac{1}{\text{NEP}} \sqrt{\frac{A_d}{1 \text{ cm}^2}}$$

$$D^* (10-11\mu, 100, 1) = \frac{1}{6 \times 10^{-9}} = 1.66 \times 10^8 \text{ cm-cps}^{\frac{1}{2}}\text{-watts}^{-1}$$
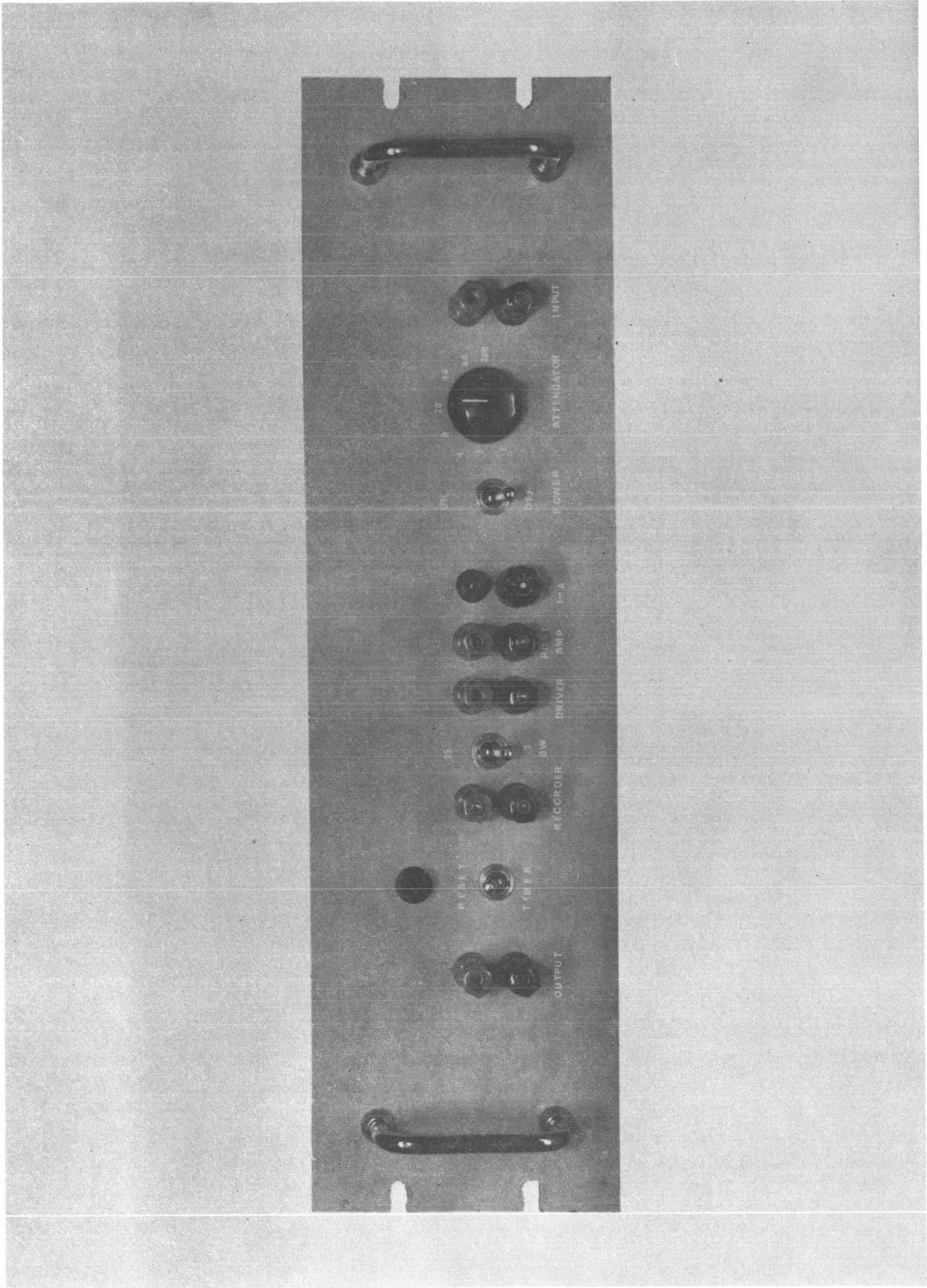
Figure I-2-1  LOW FREQUENCY SPECTRUM ANALYZER
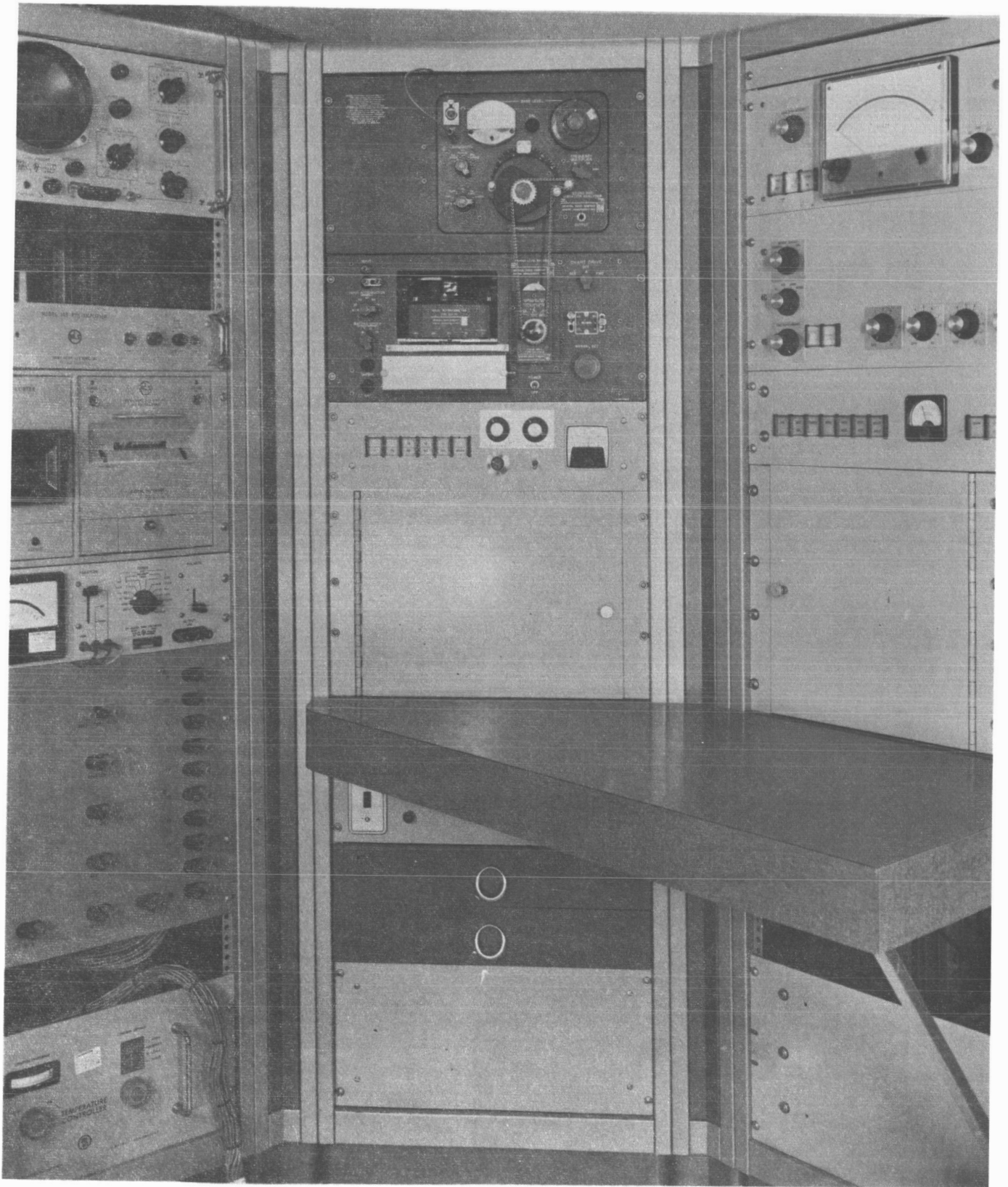
Figure I-2-2  DETECTOR TEST SET
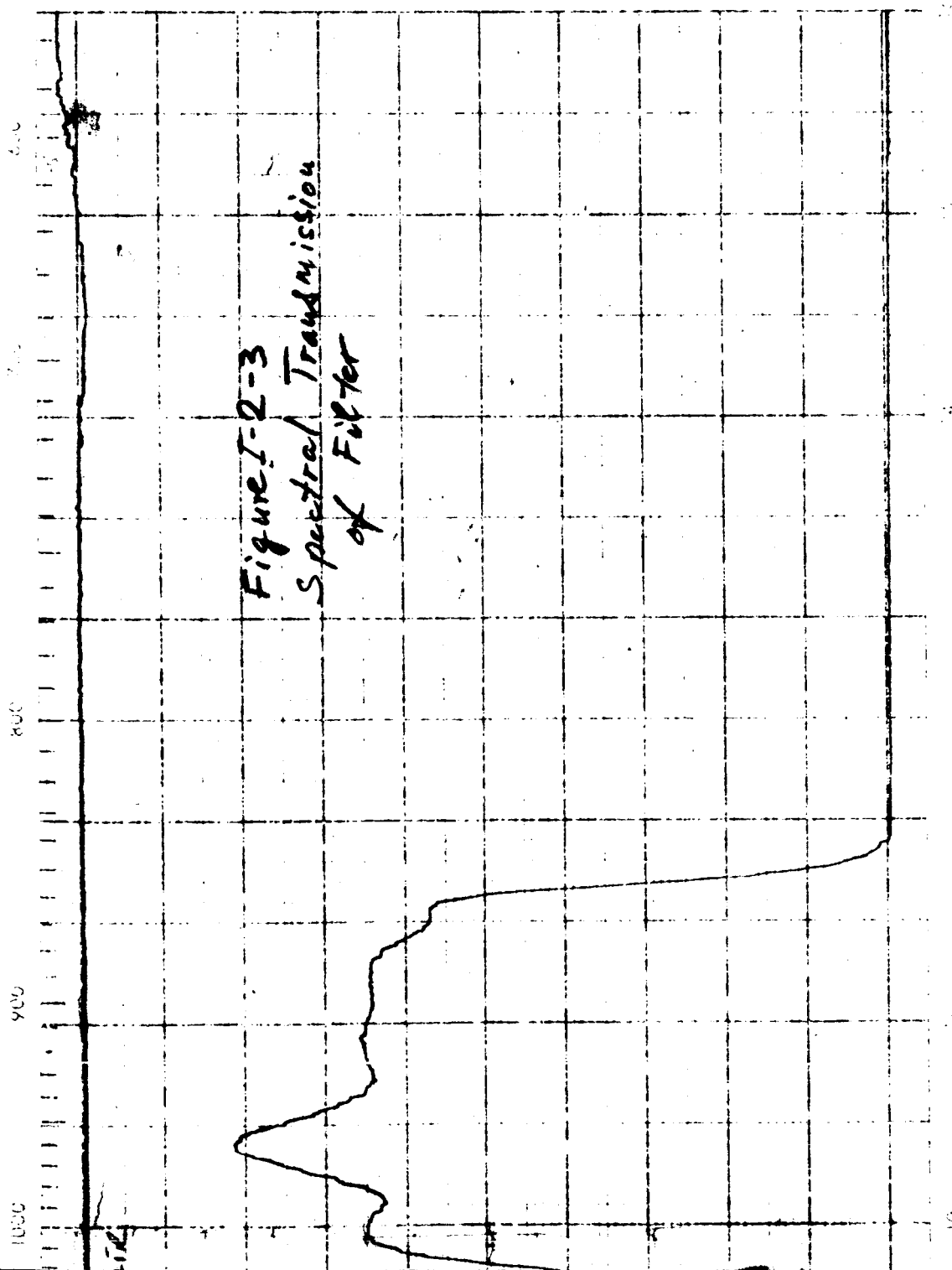
SPECTRUM NO $\underline{IR\ 2525}$

DATE $\underline{11\ July\ 1700}$

SAMPLE $\underline{WPB\ FILTER:\ TWO}$
$\underline{(2)\ ELEMENT\ COMPOSITE}$

$\underline{PL.C-19984/ALL}$

SOURCE $\underline{A.\ TEWEATL}$

STRUCTURE _____

$\underline{EACH\ ELEMENT\ 1^{in}\ DIA.}$
$\underline{\times\ 1\ mm\ t.}$

PATH _____

SOLVENT _____

CONCENTRATION _____

PHASE _____

DRAWINGS $\underline{W-09830-9+}$
$\underline{L-09700-9B.}$

$\underline{2034-45.}$

ANALYSIS _____

**Beckman**
INFRARED

SPECTRUM

Figure 2-3
Spectral Transmission
of Filter

100% η: 4.72
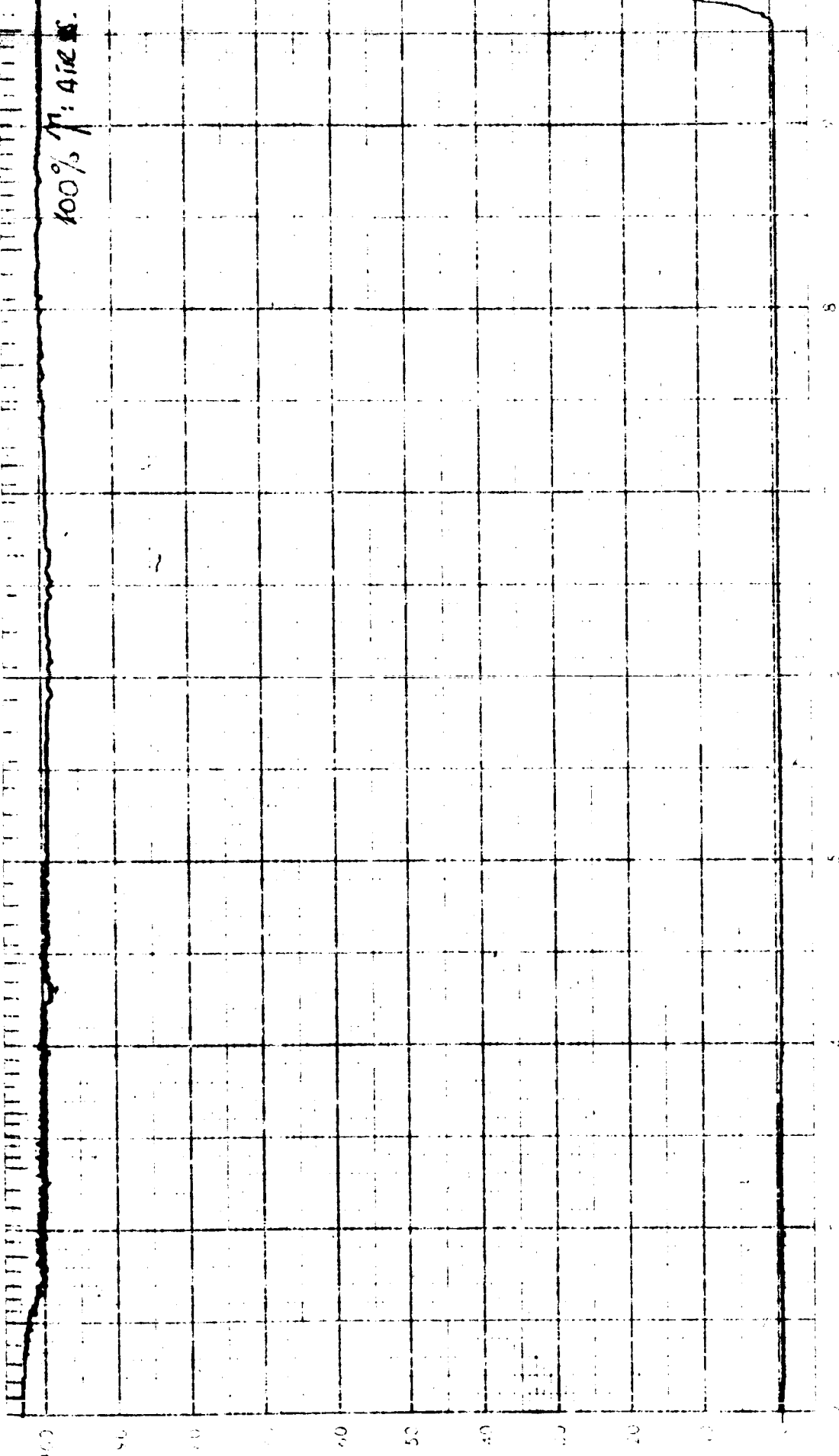
POL-16984 (9.8-11.7μ) IRT 2525
<u>BLACK</u> CHOPPER TEMP. 300°K
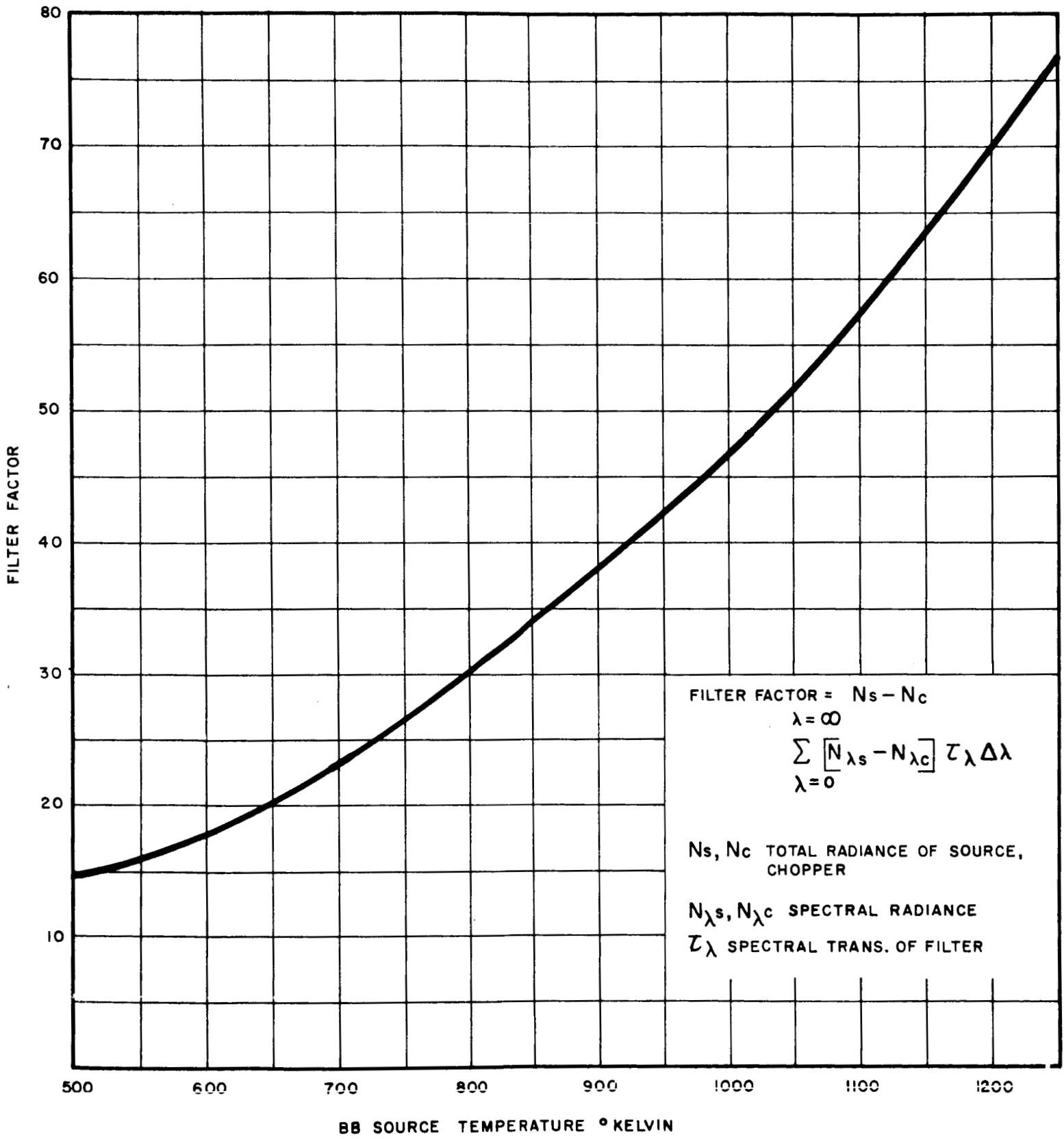


Figure I-2-4 FILTER FACTOR vs. SOURCE TEMP. FOR PROJECT 2034 FILTER
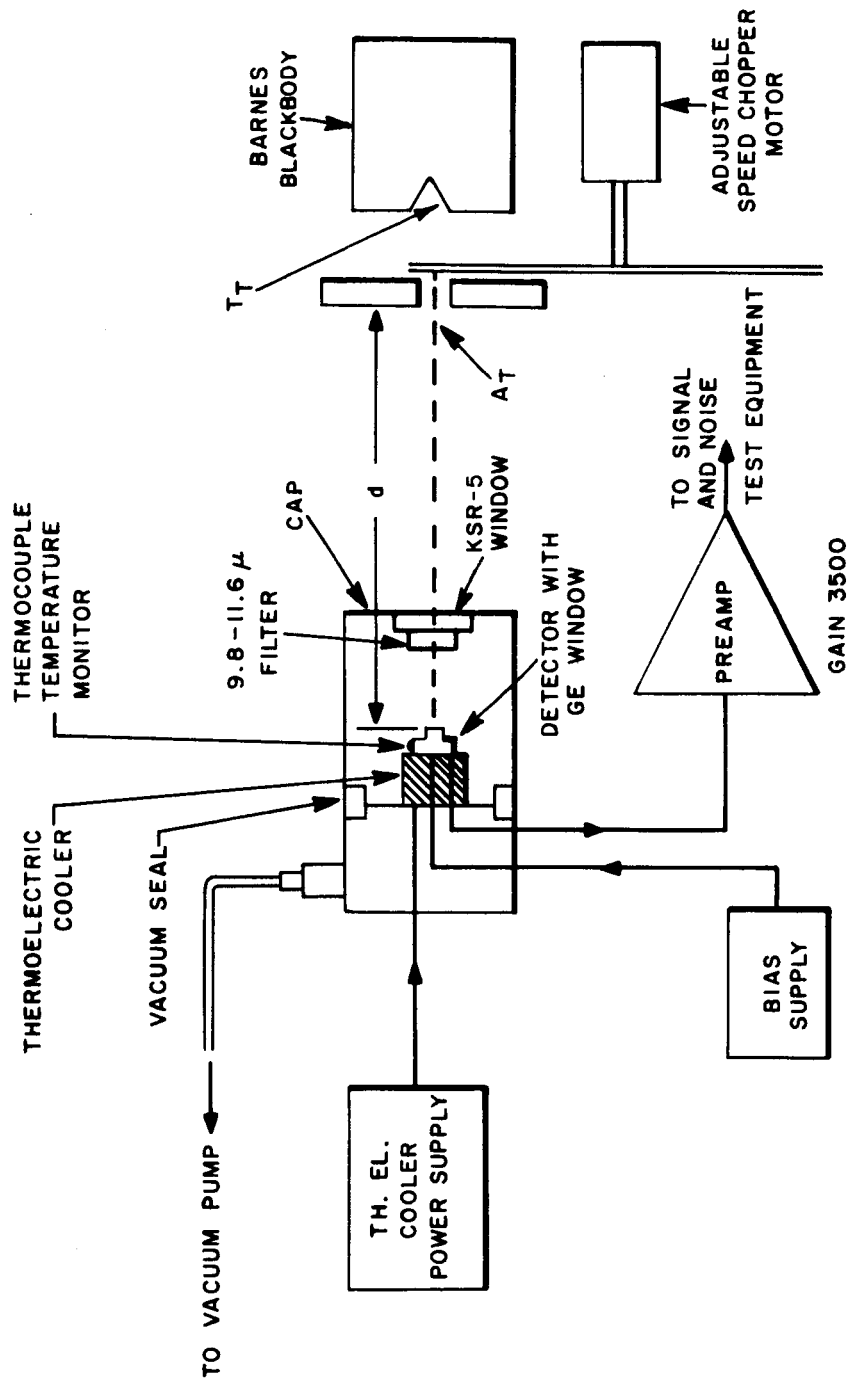
Figure I-2-5 DETECTOR TEST SET-UP

## 3. PRESENTATION OF DATA

Since the voluminous tables of measurements made on this program would tend to confuse rather than to enlighten the reader, this Section consists of a description of the types of data available as a result of our effort rather than the data itself.

Complete data sheets are attached, for illustrative purposes, on a single detector (BEC 5826). From this data one may derive the appropriate curves showing the relationships between various parameters under particular operating conditions, for this detector. See Figures I-3-1, I-3-2, I-3-3 and I-3-4. In Figure I-3-3, we have plotted the detectivity as a function of frequency for room temperature at a bias level of 0.6 $V_{pk}$ and for -25°C at a bias level of 0.8 $V_{pk}$. Figure I-3-4 shows detectivity as a function of temperature. As discussed in Section 2, the Noise Equivalent Power and detectivity determinations are based on measurements in which the power incident on the detector is $8 \times 10^{-8}$ watt, limited to the 9.8$\mu$ to 11.7$\mu$ spectral interval.

Curves showing D* and Relative Frequency Response and D* vs Ambient Temperature are included for six additional detectors in Figures I-3-5 through I-3-16. Figures I-3-5 through I-3-10 are for thin detectors and Figures I-3-11 through I-3-16 are for standard thickness detectors.

Considerably more graphical data could be presented by showing the performance of all test samples at other bias levels, other temperatures, etc. However, we have determined that conditions departing widely from the ones which we have recommended are not desirable. For example, higher bias values than 0.8 $V_{pk}$ bring about diminishing returns and entail considerable danger of detector destruction unless certain precautions are taken in the circuitry used. Obviously, much additional data and many relationships between the various parameters could be derived. For example, one could plot curves showing improvement factor as a function of operating temperature alone or bias level alone. One could plot the time constant directly as a function of detector temperature, noise as a function of temperature, etc. Should certain special items of information be required regarding characteristics which we have not included here, we will gladly furnish the data on request.

# BARNES ENGINEERING COMPANY

30 COMMERCE ROAD    STAMFORD, CONNECTICUT

# IMMERSED THERMISTOR DETECTOR

TYPE NO. _Ge - Se - E_        SERIAL NO. BE- _5826_



BOLOMETER SIGNAL CONNECTIONS

*Recommended diagonal signal connections.
(Not connected in detector)



BOLOMETER ELECTRICAL CIRCUIT

$V_A = V_C$  $R_A = R_C$  $R_G \gg R_A$
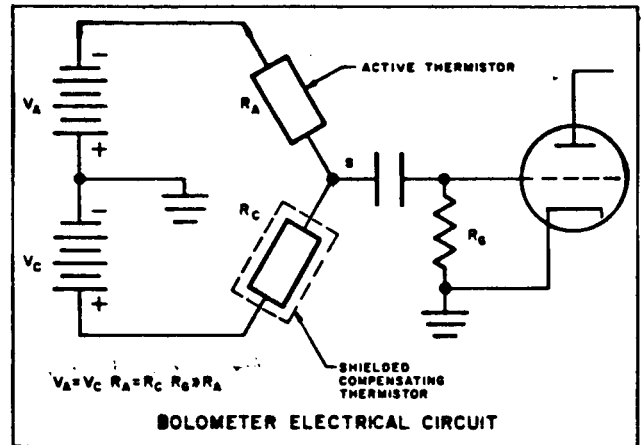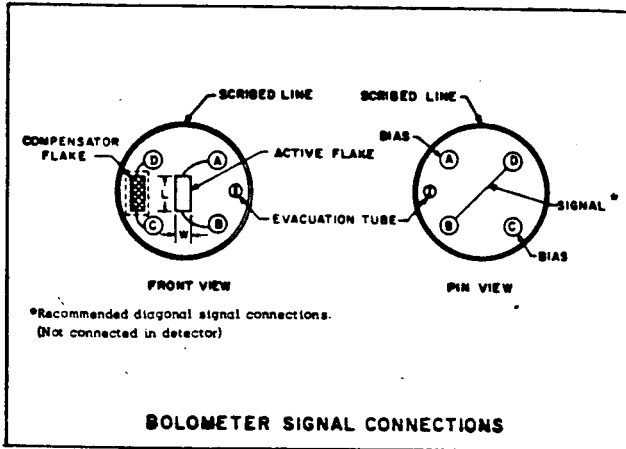
PEAK VOLTAGE AT 25°C:

    Active Flake (A and B)___ _85.5_ ___Volts
    Compensator Flake (C and D)_ _80.6_ _Volts

MAXIMUM RECOMMENDED BOLOMETER BIAS:

    Plus and Minus___ _48.3_ ___Volts at 25°C

FLAKE ACTIVE AREA:

    Length (L)___ _0.2_ ___millimeters
    Width (W)___ _0.2_ ___millimeters
    Area___ _0.04_ ___square millimeters
    ☒ EVACUATED  ☐ HERMETICALLY SEALED

LENS MATERIAL_ _GERMANIUM_ ___
ANTI-REFLECTION COATING PEAKED AT_ _—_ _Microns

LENS AND BASE DIMENSIONS:

    r    = _____millimeters

    t    = _~1.0_ ___millimeters

    flake
    centering = ± _____millimeters
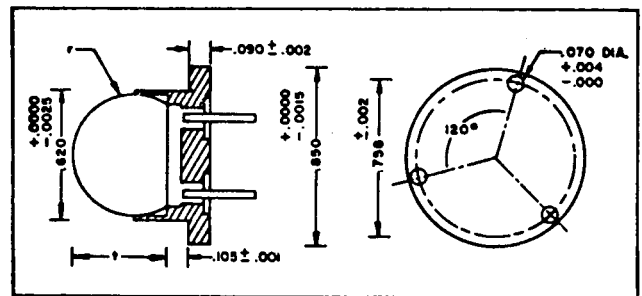


| FLAKE | RESPONSIVITY (See Note A) | TIME CONSTANT Milliseconds | RESISTANCE Megohms, 25°C | NOISE (See Note B) |
|-------|---------------------------|----------------------------|--------------------------|--------------------|
| ACTIVE A and B | 902 v/w | 1.1 | 0.518 | 0.854 μv |
| COMP. C and D | | | 0.533 | |

U.S. Patent Nos: 2983887; 2983888; 2963673; 3109097        — OVER —

_v. 15 F_

**NOTE A:** Responsivity of the active flake in VOLTS RMS PER AVERAGE WATT. Measured at 25°C, in 1-100 cps electrical bandwidth, with 470°K blackbody radiation, square-wave chopped at 15 cps, incident on the immersion lens and with an applied bias voltage of ___45___ volts per flake. Irradiance on immersion lens about 2 microwatts peak-to-peak per square millimeter. When active flake is used with an equal-resistance compensator flake, its responsivity at the signal junction is one-half the given value.

**NOTE B:** RMS noise at signal junction (matched flake pair), measured in 5-100 cps electrical bandwidth.

$$NOISE = \sqrt{(NOISE\ w/BIAS)^2 - (EQUIP.\ NOISE)^2}$$

DATA BY: _____  DATE: 1/4/67

CHECKED BY: _____  DATE: 1/4/67

**DET. # 5826**

**TYPE:** GE-SE-E
**FLAKE MAT. # 2**

**IMMERSED ON** Flat   $r = 7.5$ mm   $t = \sim 1.$ mm SE 80-20t $= \mu$
**SIZE:** $0.2 \times 0.2$   $t =$ Thin
$R_A = 518K$   $R_C = 533K$

**FILTER:** OCLI 2034

ww **RESISTORS:**   K $\Omega$

$N_{GG}$ @ 25 cps:
100 cps:
200 cps:

**TEST SET:**

$N_o$   @ 25 cps:
100 cps:
200 cps:

$N_{max}$ (     ) @ 25 cps:
100 cps:
200 cps:

**TEMP.** 25.2°C

$V_p =$ A $= 85.5$ V.
         C $= 80.6$ V.

| f | .6 Vp = ±48.5 V | | | .4 Vp = ±32 | | | .8 Vp = ±64.5 | | | .9 Vp = ±72 V | | |
|---|---|---|---|---|---|---|---|---|---|---|---|---|
| | $N_o$ | $N_B$ | Signal | $N_o$ | $N_B$ | Signal | $N_o$ | $N_B$ | Signal | $N_o$ | $N_B$ | Signal |
| .04 | | 300 mV | | | | | | 450 mV | | | | |
| .1 | | 120 | | | | | | 190 | | | | |
| .2 | | 40 | | | | | | 64 | | | | |
| .5 | | 9.5 | | | | | | 15 | | | | |
| 1 | | 4.8 | | | | | | 7 | | | | |
| 4 | | 1.9 | | | | | | 2.5 | | | | |
| 15 | | 1.28 | | | | | | 1.25 | | | | |
| 20 | .58 mV | 1.05 mV | 192 mV | | 1 mV | 134 mV | | 1.05 mV | 207 mV | | 1.16 mV | 223 mV |
| 40 | .55 mV | 0.9 | 190 | | 1 mV | 132 | | 1.0 | 203 | | 1.15 | 220 |
| 100 | .52 | .85 | 168 | | .8 | 117 | | .72 | 188 | | .85 | 202 |
| 200 | .48 | .65 | 123 | | .6 | 85 | | .67 | 147 | | .75 | 165 |
| 300 | .48 | .6 | 102 | | .55 | 70 | | .64 | 123 | | .75 | 140 |

**H. P.** Wave Analyzer 15 - 300 cps.
LFS 0.04 - 100

DET. # 5826

TYPE:                          t =     SE      t = µ
FLAKE MAT. #2                  R_A =   R_C =

IMMERSED ON                    r = Thin
SIZE:                          t = Thin

FILTER:        ww RESISTORS:   K Ω

               N_GG @ 25 cps:
                    100 cps:
                    200 cps:

               N_o  @ 25 cps:
                    100 cps:
                    200 cps:

TEST SET:

Vp = 123       N_max (   ) @ 25 cps:
                         100 cps:
                         200 cps:

TEMP.  0°C

| f | .6 Vp = ±74 | | | .4 Vp = ±50 V | | | .8 Vp = ±98.5 | | | .9 Vp = ±110 | | |
|---|---|---|---|---|---|---|---|---|---|---|---|---|
| | $N_o$ | $N_B$ | Signal | $N_o$ | $N_B$ | Signal | $N_o$ | $N_B$ | Signal | $N_o$ | $N_B$ | Signal |
| .04 | | 250 mV | | | | | | 350 mV | | | | |
| .1 | | 100 | | | | | | 150 | | | | |
| .2 | | 50 | | | | | | 77 | | | | |
| .5 | | 13 | | | | | | 25 | | | | |
| 1 | | 6.5 | | | | | | 8.5 | | | | |
| 4 | | 2.5 | | | | | | 3.2 | | | | |
| 15 | | 1.7 | | | | | | 2.2 | | | | |
| 20 | 900 mV | 1.35mV | 365 mV | | 1.2 mV | 255 mV | | 1.55 mV | 420 mV | | 1.7 mV | 460 mV |
| 40 | 930 | 1.3 | 360 | | 1.2 | 250 | | 1.4 | 415 | | 1.5 | 450 |
| 100 | 900 | 1.2 | 320 | | 1.2 | 225 | | 1.25 | 380 | | 1.2 | 420 |
| 200 | 780 | 1.1 | 243 | | 1.0 | 160 | | 1.0 | 310 | | 1.2 | 340 |
| 300 | 750 | 0.9 | 218 | | 1.0 | 140 | | 1.0 | 283 | | 1.1 | 325 |

H. P. Wave Analyzer  15 - 300 cps.

LFS  0.04 – 100

DET. # 5826

TYPE:
FLAKE MAT. # 2

TEST SET:

TEMP.  −25°C

Vp = 214

IMMERSED ON
SIZE:

FILTER:

t =          SE          t = μ
$R_A$ =     $R_C$ =

r = Thin
t = Thin

ww RESISTORS:                K Ω
$N_o$      @ 25 cps:
               100 cps:
               200 cps:

$N_{GG}$ @ 25 cps:
               100 cps:
               200 cps:

$N_{max}$ (      )  @ 25 cps:
                           100 cps:
                           200 cps:

| f | .6 Vp = ±128 | | | .4 Vp = ±83 V. | | | .8 Vp = ±171 | | | .9 Vp = ±190 | | |
|---|---|---|---|---|---|---|---|---|---|---|---|---|
| | $N_o$ | $N_B$* | Signal | $N_o$ | $N_B$ | Signal | $N_o$ | $N_B$ | Signal | $N_o$ | $N_B$ | Signal |
| .04 | | 250 mV | | | | | | 275 mV | | | | |
| .1 | | 110 | | | | | | 155 | | | | |
| .2 | | 54 | | | | | | 75 | | | | |
| .5 | | 20.5 | | | | | | 32 | | | | |
| 1 | | 10.5 | | | | | | 12 | | | | |
| 4 | | 3.5 | | | | | | 4.6 | | | | |
| 10 | | 2.5 | | | | | | 2.6 | | | | |
| 20 | 2.0 | 2.15 mV | 635 mV | | 2.0 mV | 445 mV | | 2.4 mV | 800 mV | | 3.0 mV | 870 mV |
| 40 | | 2.1 | 625 | | 2.0 | 440 | | 2.25 | 800 | | 2.5 | 870 |
| 100 | | 2.0 | 620 | | 1.8 | 425 | | 2.05 | 800 | | 2.2 | 850 |
| 200 | | 2.0 | 560 | | 0.95 | 375 | | 1.7 | 700 | | 2.0 | 770 |
| 300 | | 2.0 | 510 | | 1.0 | 340 | | 1.35 | 600 | | 1.5 | 680 |

**H. P. Wave Analyzer 15 - 300 cps.**
LFS 0.04 − 100~

* All normalized to 7-1/2 Hz bandwidth

DET. # 5826    TYPE:    FLAKE MAT. # 2     DATE: 1-17-67

| | |
|---|---|
| **DET.** # 5826 | |
| **TYPE:** | |
| **FLAKE MAT.** # 2 | |
| **FILTER:** | |
| **TEST SET:** | |
| **TEMP.** -35.2°C    Vp = 208 V. | |

**IMMERSED ON**  
**SIZE:**  
$N_{GG}$ @ 25 cps: / 100 cps: / 200 cps:

t =    SE    t = μ  
r =  
$R_A$ =    $R_C$ =  
t = Thin

ww RESISTORS:    K Ω  
$N_o$ @ 25 cps: / 100 cps: / 200 cps:

$N_{max}$ (   ) @ 25 cps: / 100 cps: / 200 cps:

| f | .6 Vp = ±162 | | | .4 Vp = ±83 | | | .8 Vp = ±165 | | | .9 Vp = ±187 | | |
|---|---|---|---|---|---|---|---|---|---|---|---|---|
| | $N_o$ | $N_B$ | Signal | $N_o$ | $N_B$ | Signal | $N_o$ | $N_B$ | Signal | $N_o$ | $N_B$ | Signal |
| .04 | | 160 mV | | | | | | | | | | |
| .1 | | | | | | | | | | | | |
| .2 | | | | | | | | | | | | |
| .5 | | | | | | | | | | | | |
| 1 | | 15.4 | | | | | | | | | | |
| 4 | | 6.0 | | | | | | | | | | |
| 15 | | | | | | | | | | | | |
| 20 | 3.0 | 3.4 | 695 | | 2.5 mV | 485 mV | | 4.2 mV | 920 mV | 5 mV | | 1000 mV |
| 40 | | 3.4 | 685 | | 2.5 | 475 mV | | 4.4 | 910 | 5 | | 980 |
| 100 | | 3.2 | 675 | | 2.2 | 465 | | 2.9 | 910 | 3.5 | | 980 |
| 200 | | 3.0 | 620 | | 1.5 | 410 | | 2.7 | 800 | 3.5 | | 900 |
| 300 | | 3.0 | 570 | | 1.0 | 390 | | 1.3 | 690 | 2 | | 750 |

**H. P. Wave Analyzer 15 - 300 cps.**  
LFS 0.04 - 100~

Figure I-3-I  RELATIVE OUTPUT vs. FREQUENCY DETECTOR 5826
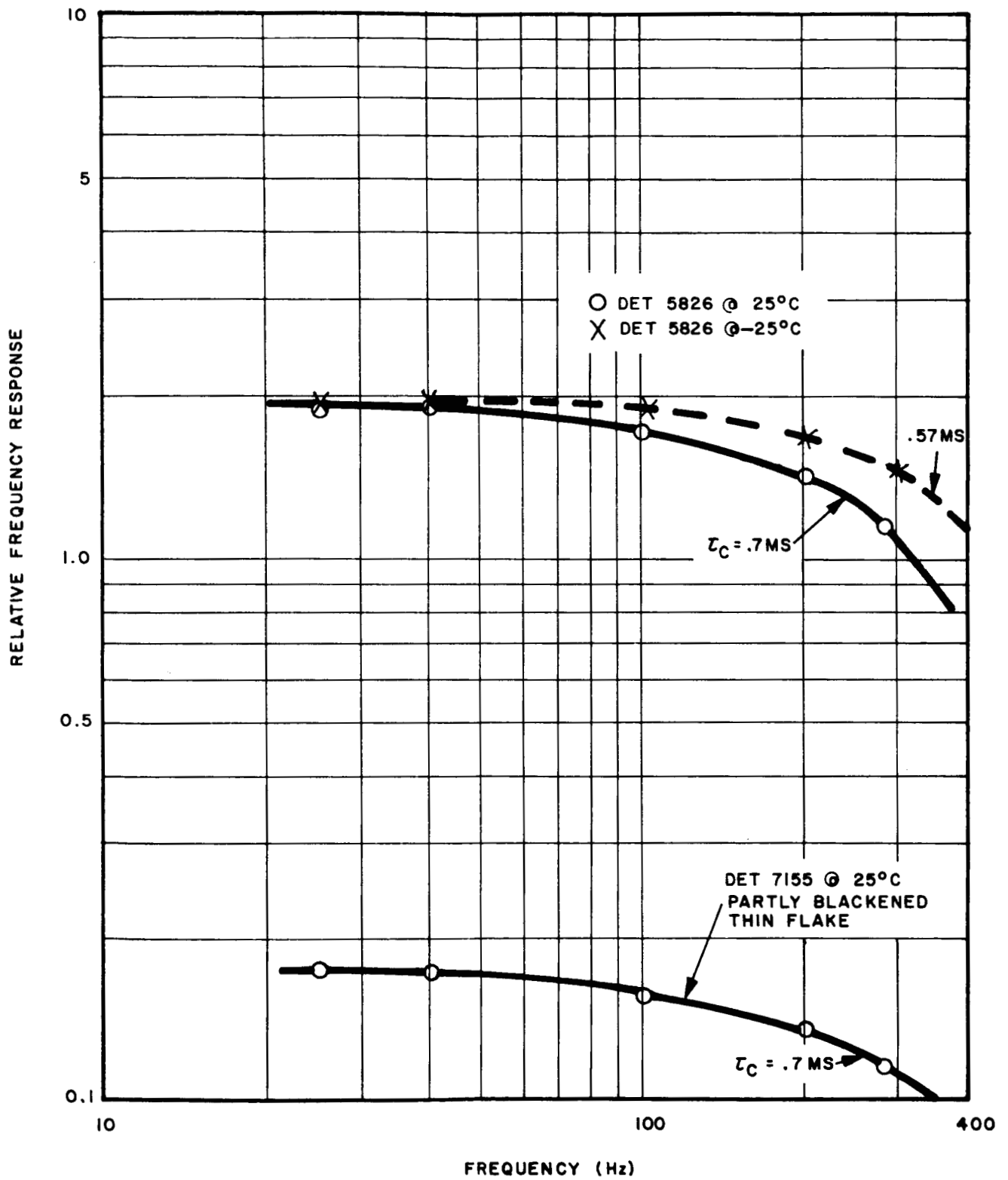
Figure I-3-2  TIME CONSTANT OF DET 5826, THIN FLAKE, PARTIALLY BLACKENED-
0.8V PEAK
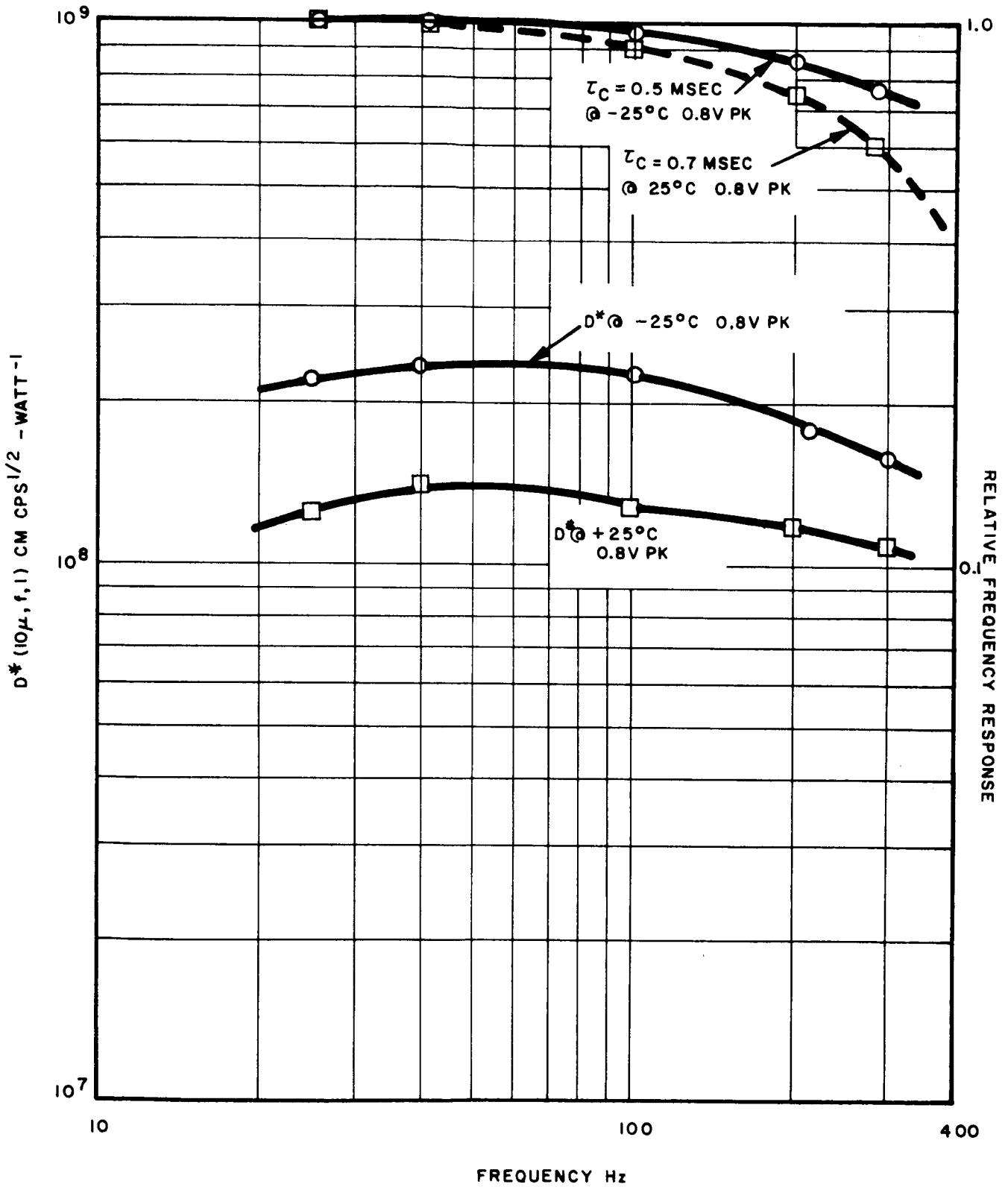
Figure I-3-3 D* AND RELATIVE FREQUENCY RESPONSE OF IMMERSED DETECTOR BEC 5826 0.2 mm x 0.2 mm, THIN FLAKE WITH ONE COAT OF APB
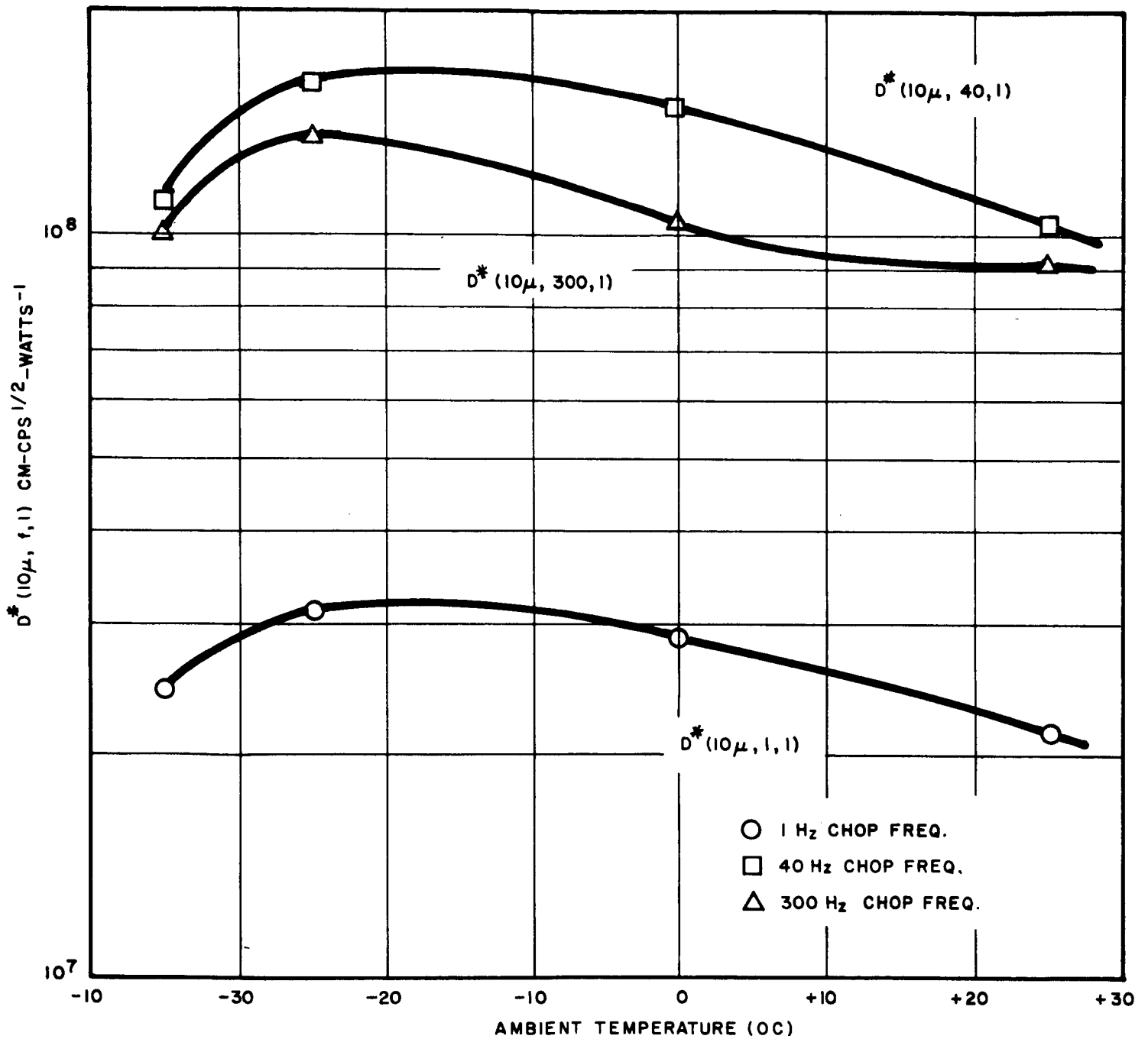
Figure I-3-4 D* vs. AMBIENT TEMPERATURE FOR DETECTOR 5826 OPERATED AT 0.6 PEAK BIAS
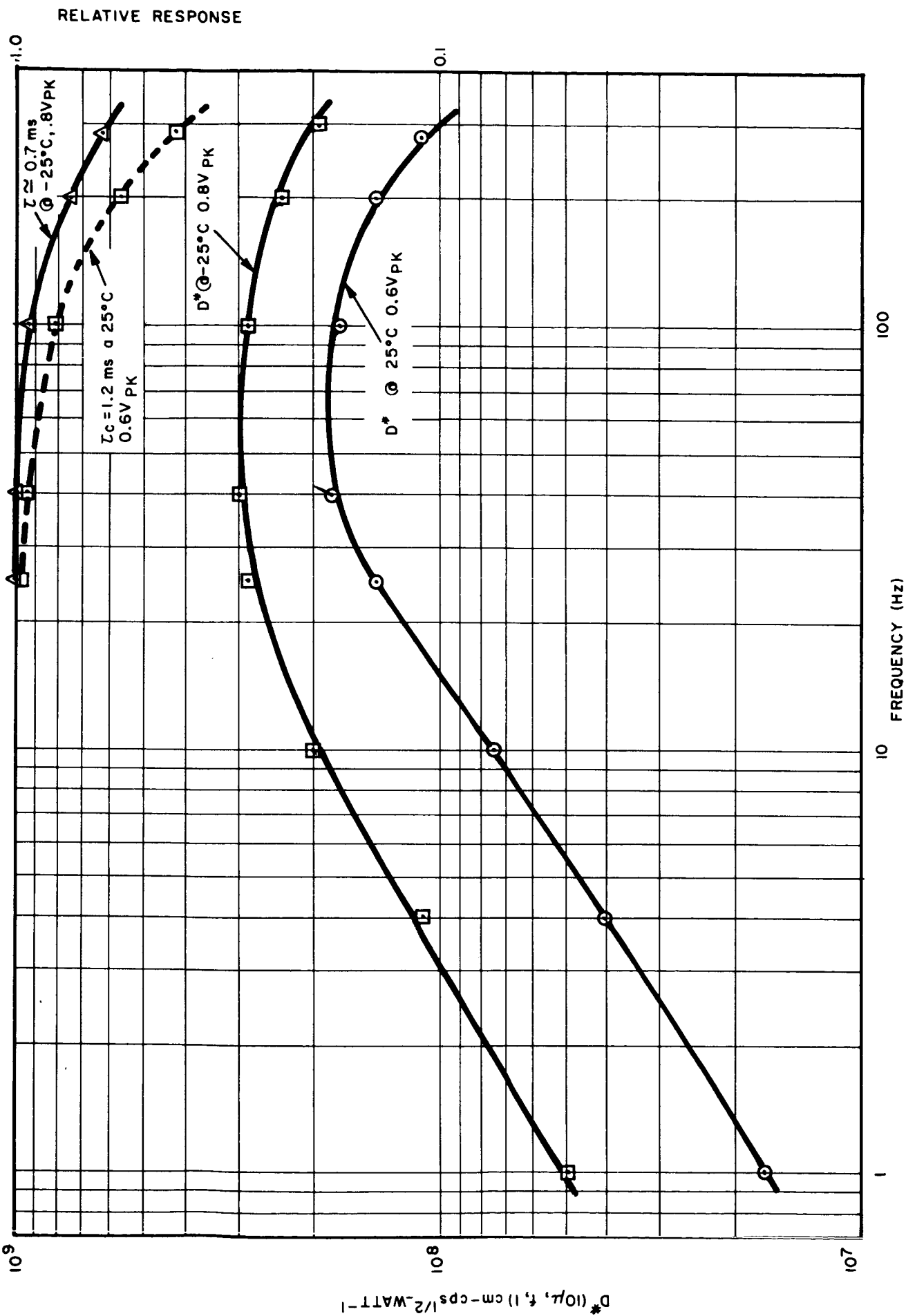
RELATIVE RESPONSE

Figure I-3-5   D* AND RELATIVE FREQUENCY RESPONSE OF DETECTOR # 7140
THIN, FULLY BLACKENED
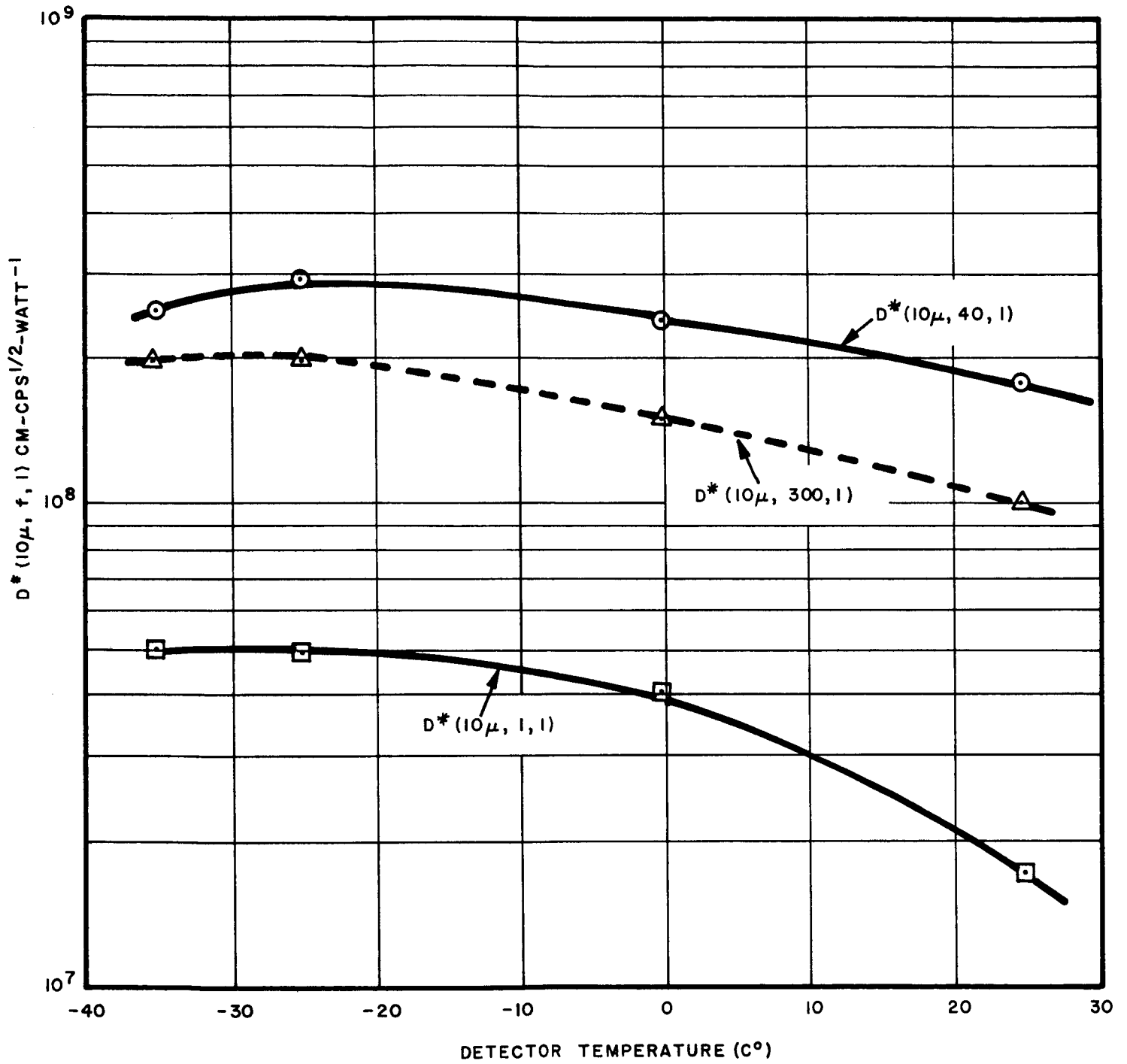
Figure I-3-6   DETECTIVITY AS A FUNCTION OF DETECTOR TEMPERATURE
DETECTOR # 7140 (THICKNESS-8$\mu$)

RELATIVE FREQUENCY RESPONSE

$\tau_c = 730\,\mu s$ @ 0°C

$\tau_c = 1.14\,ms$

$\tau_c$ @ 25°C

D*@0°C .8V$_{PK}$

D*+25°C .6V$_{PK}$

FREQUENCY (Hz)

D*(10$\mu$,f,l) CM-CPS$^{1/2}$-WATT$^{-1}$
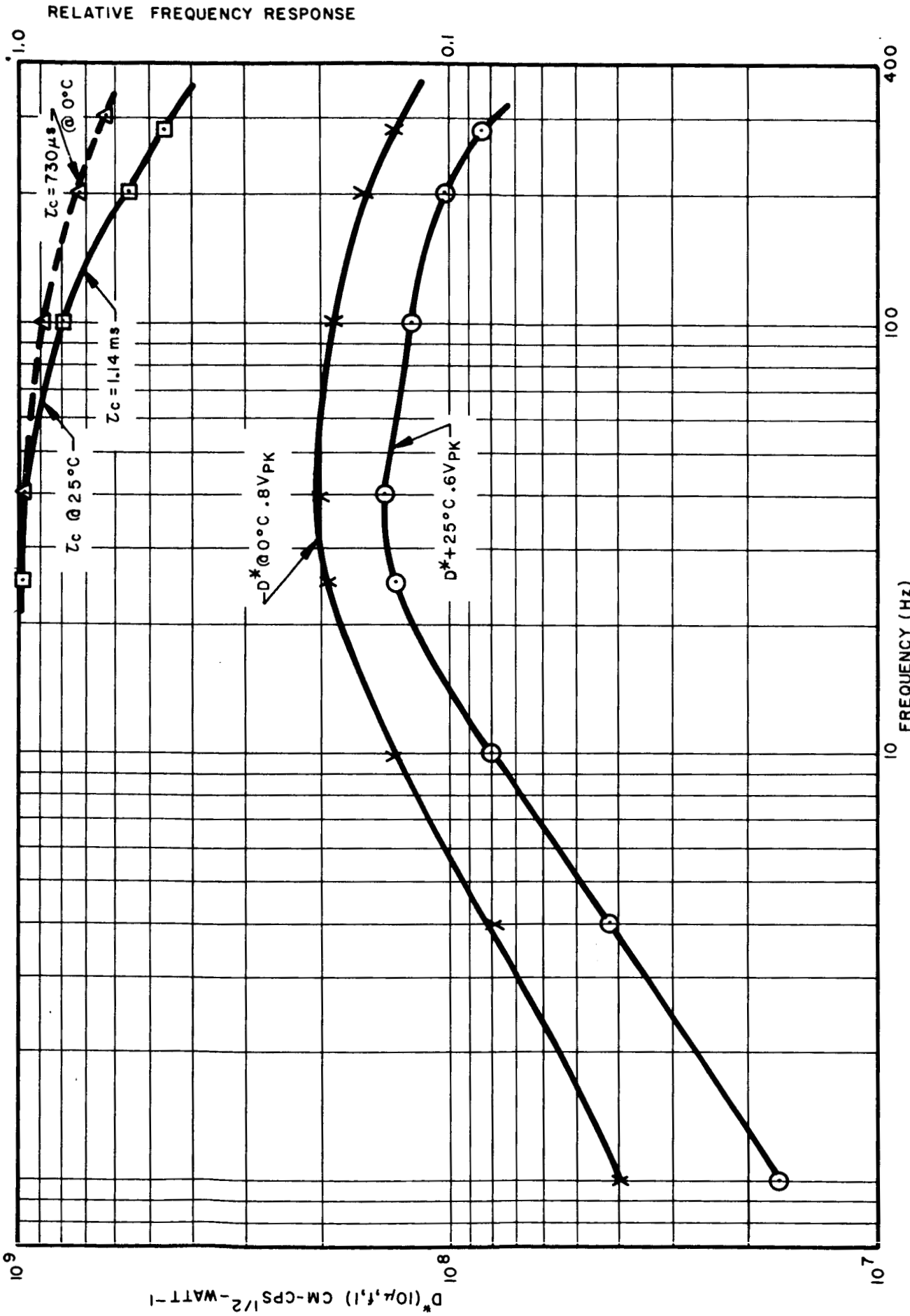
Figure I-3-7, D* & $\tau_c$ OF THIN DETECTOR # 5811, BLACKENED
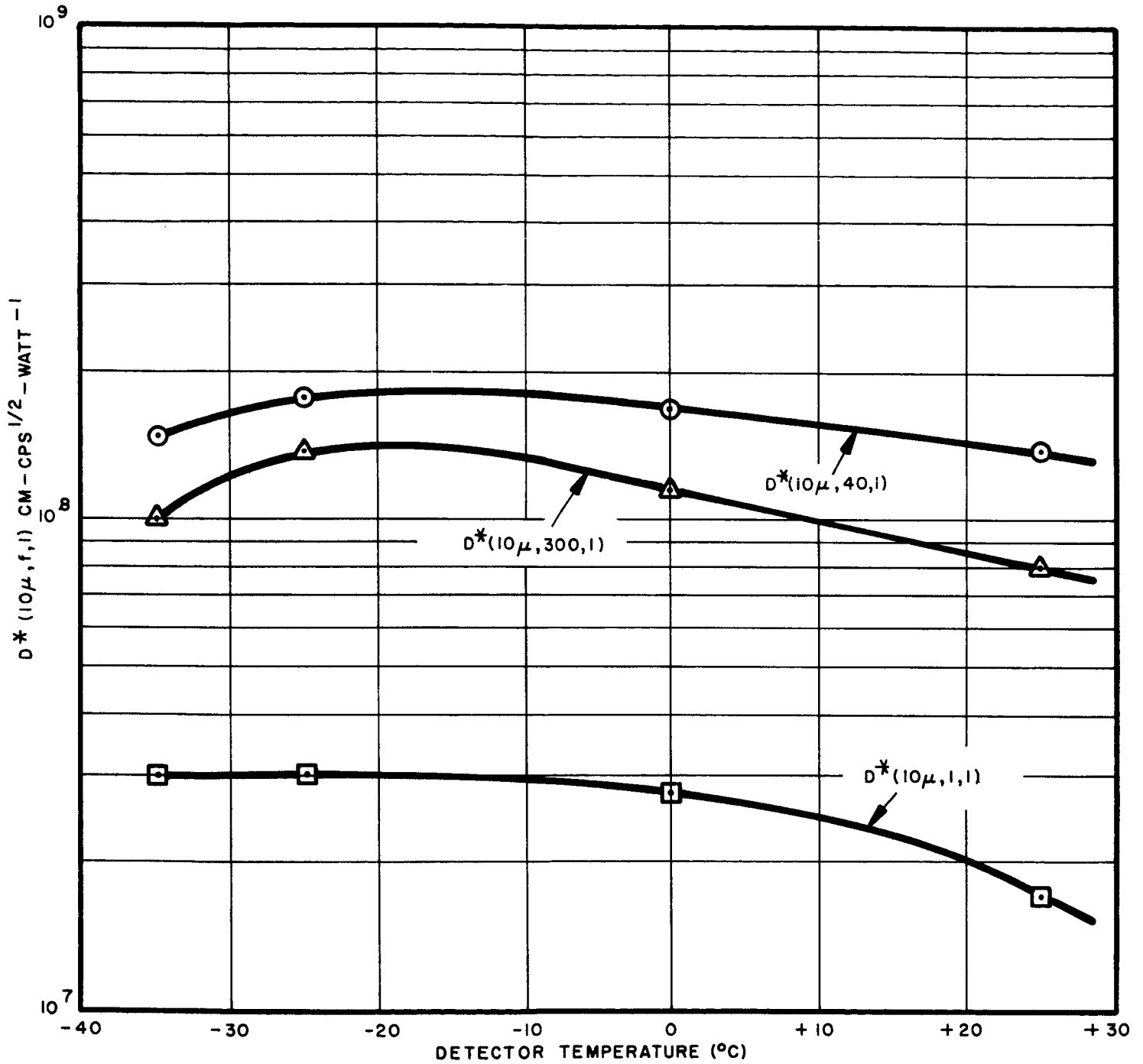
Figure 1-3-8, DETECTIVITY AS A FUNCTION OF DETECTOR TEMPERATURE FOR DETECTOR # 5811, THIN FLAKE (8 $\mu$)

RELATIVE FREQUENCY RESPONSE

$\tau_c = .5$ ms @ .8V PK

$\tau_c \simeq 0.7$ ms @ 25°C

$D^*$ @ 0°C, 0.8V PK

$D^*$ @ 25°C, 0.6 $V_{PK}$

FREQUENCY (Hz)

$D^*$ (10$\mu$, f, I) cm-cps$^{1/2}$-WATT$^{-1}$
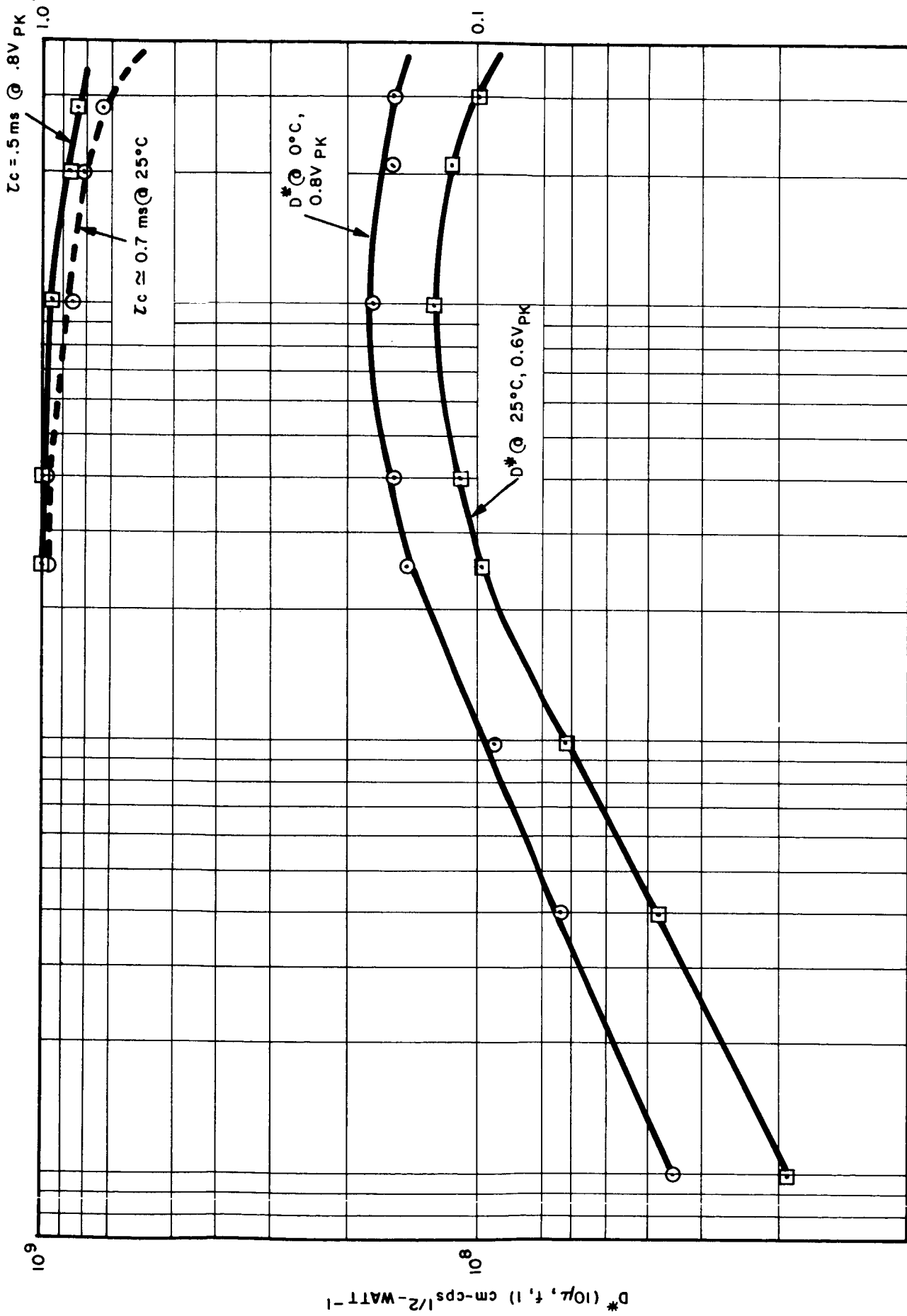
Figure I-3-9  $D^*$ AND FREQUENCY RESPONSE OF DETECTOR BEC 7155  0.2 MM x 0.2 MM
THIN FLAKE, (8 $\mu$)
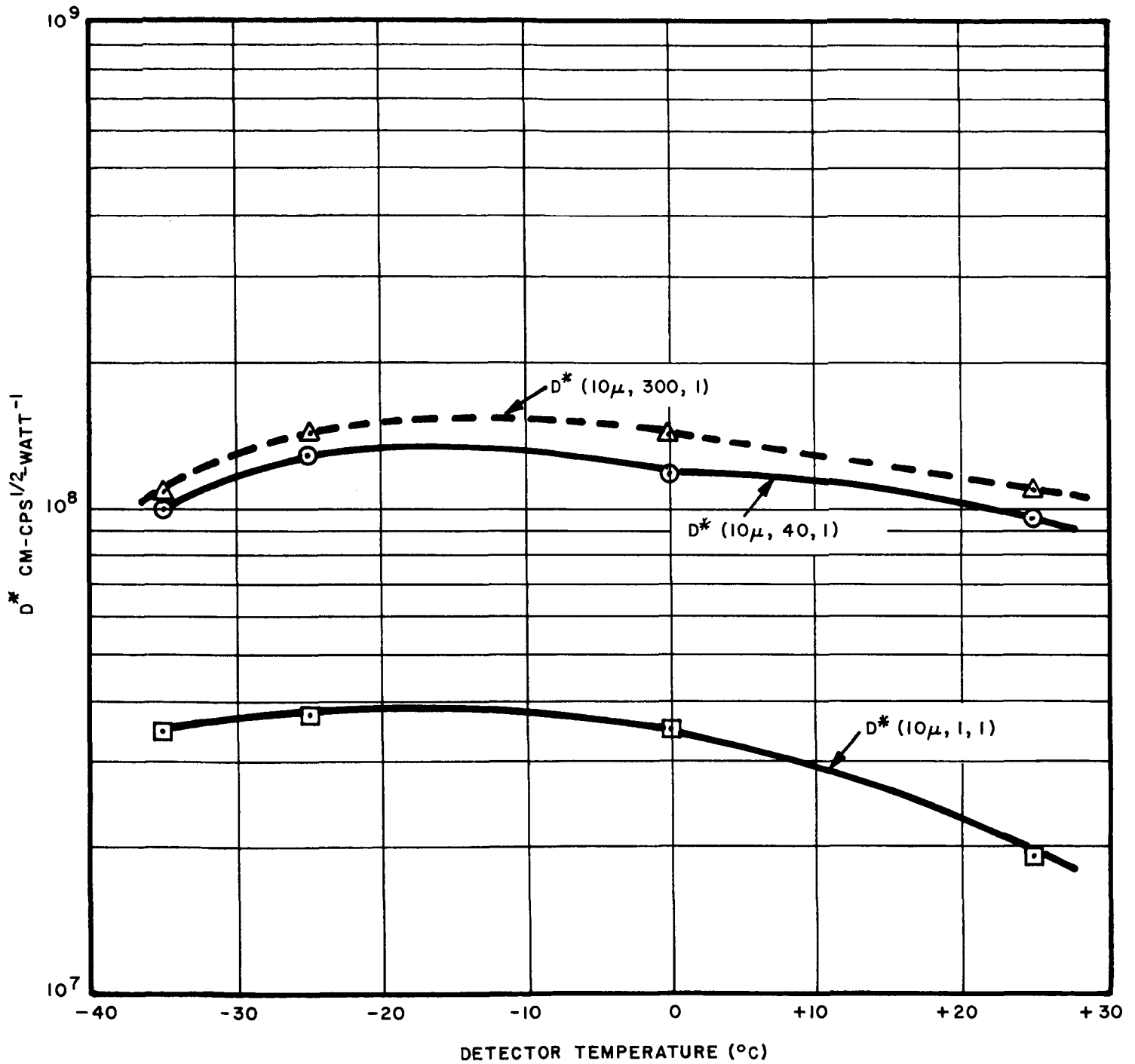
**Figure I-3-IO DETECTIVITY AS A FUNCTION OF DETECTOR TEMPERATURE FOR DETECTOR # 7155 THIN FLAKE (8μ THICKNESS)**

RELATIVE FREQUENCY RESPONSE

$\tau_c = 1.45$ M SEC @ -25°C

$\tau_c = 1.6$ M SEC @ 25°C

D* @ 25°C 0.8V PK BIAS

FREQUENCY (Hz)

D* $(10\mu, f, 1)$ CM-CPS$^{1/2}$-WATT$^{-1}$
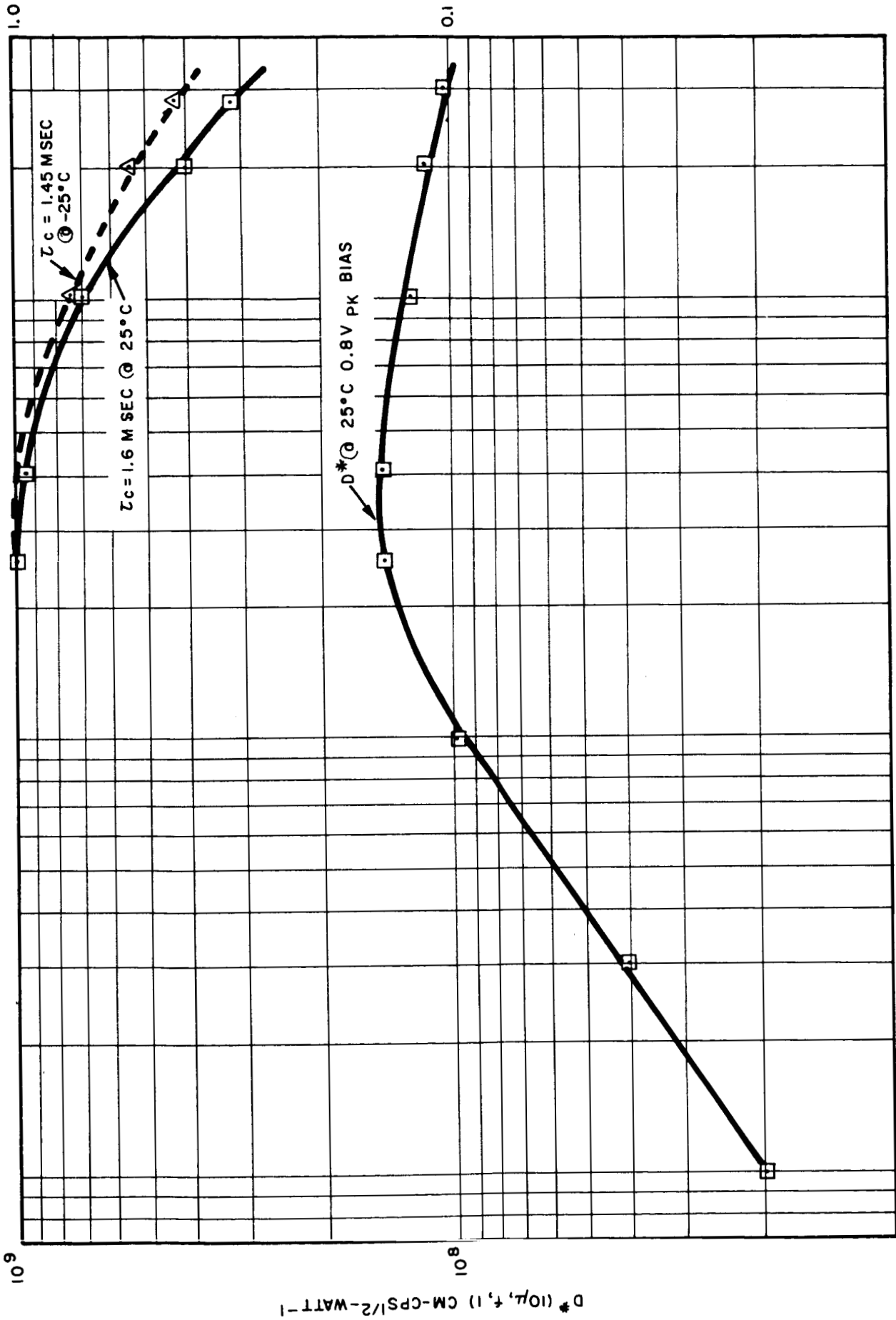
Figure I-3-11    D* AND RELATIVE FREQUENCY RESPONSE OF DETECTOR # 5853
STANDARD THICKNESS (15$\mu$)
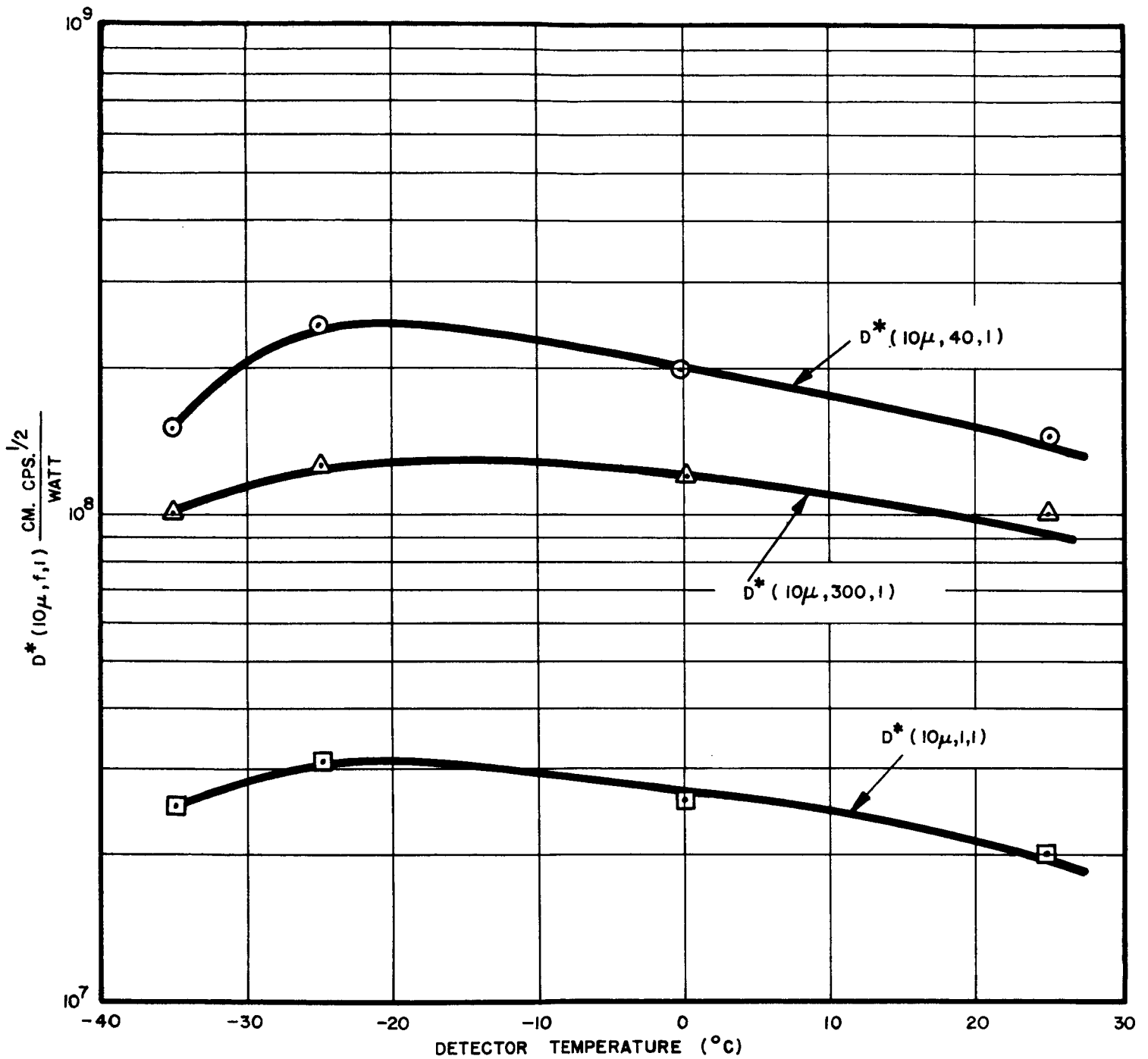
Figure I-3-12  D* VERSES DETECTOR TEMPERATURE  FOR DETECTOR NO.
5853  THICKNESS = 15 $\mu$ (STD.)
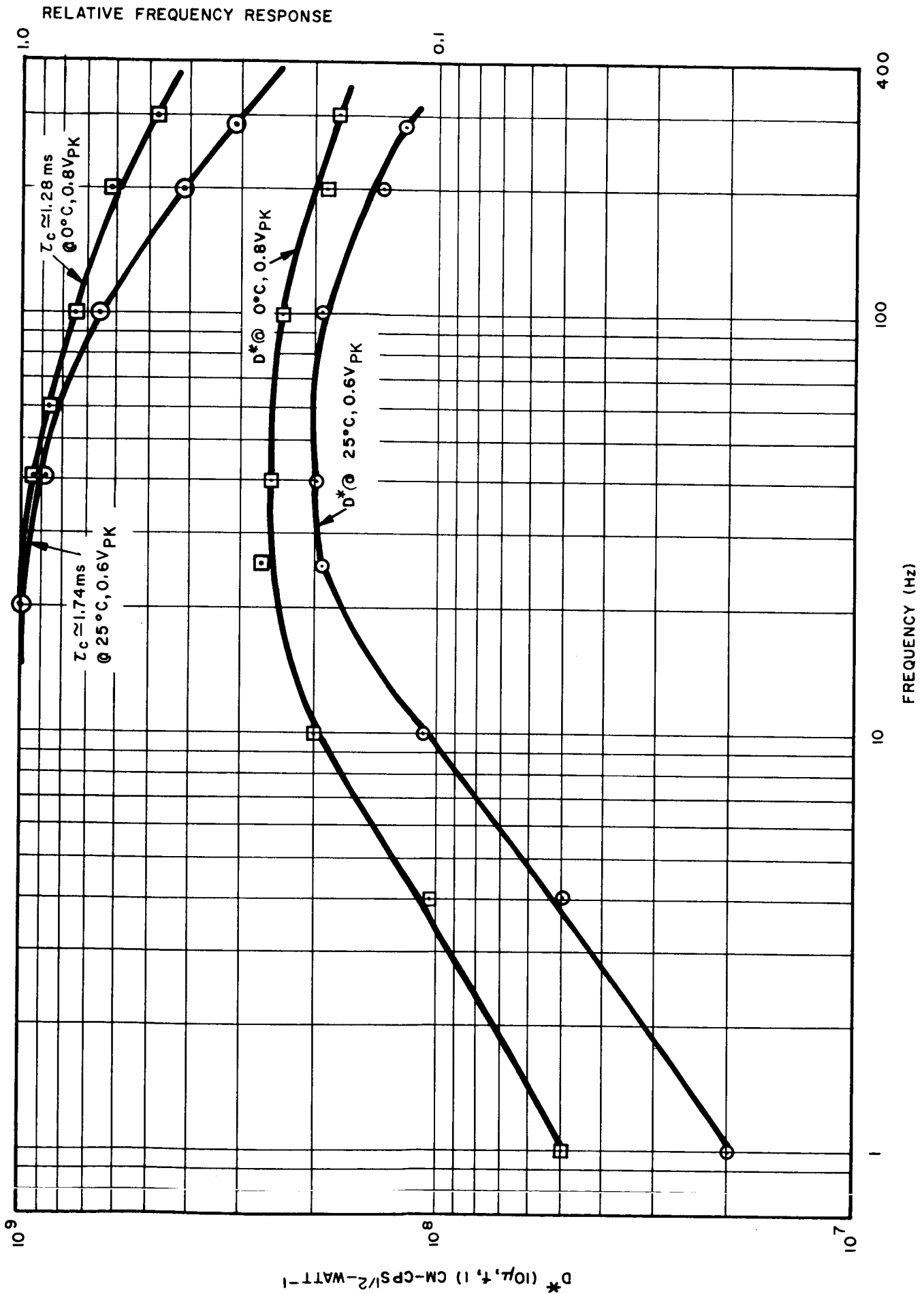
Figure I-3-I3, D* & $\tau_c$ OF DETECTOR #5807 STANDARD THICKNESS, (16$\mu$), BLACKENED
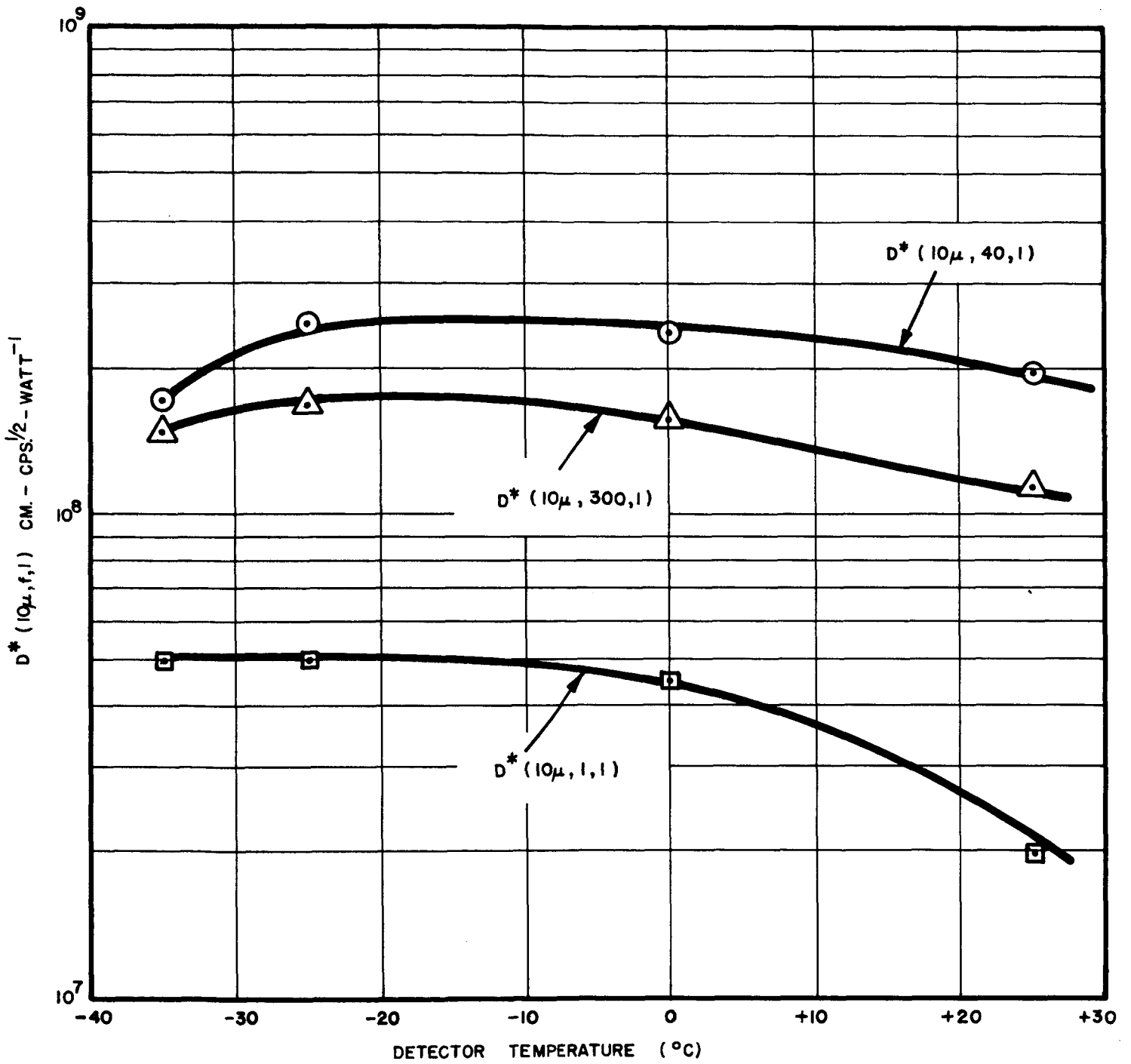
Figure I-3-I4 DETECTIVITY AS A FUNCTION OF DETECTOR TEMPERATURE
DETECTOR NO. 5807, STANDARD THICKNESS (16μ)
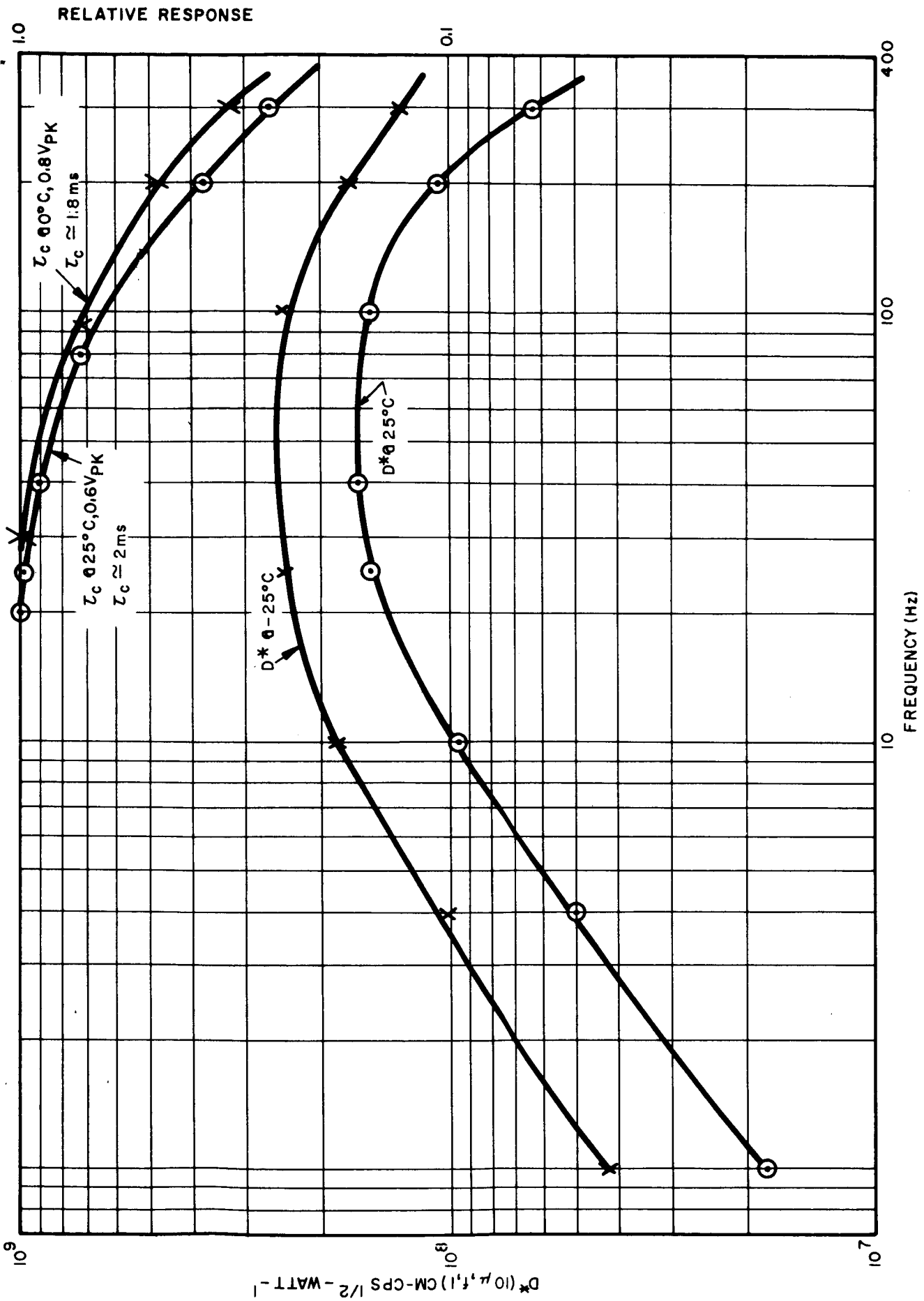
Figure I-3-15   $D^*$ & $\tau_c$ OF STANDARD THICKNESS BEC 5841, BLACKENED DETECTOR($\tau_c \simeq 2\,ms$ @ $25°C$)
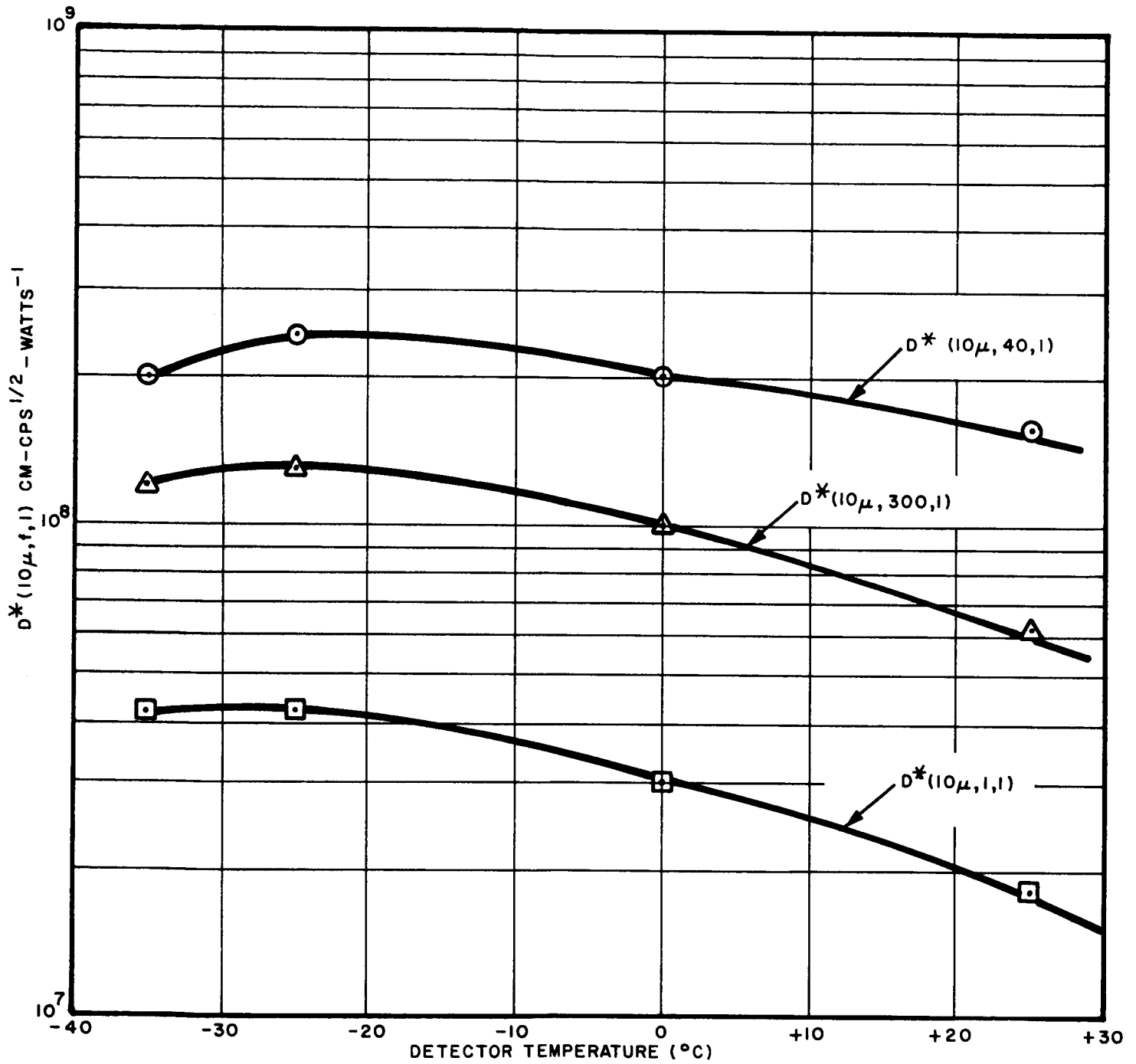
Figure I-3-16 DETECTIVITY AS A FUNCTION OF DETECTOR TEMPERATURE, DETECTOR #5841 (STANDARD THICKNESS-16$\mu$)

# 4. DISCUSSION OF DATA AND IMPROVEMENTS ACHIEVED

The results shown in this report in graphical and tabular form clearly indicate that definite improvements have been made in detector sensitivity for the particular application of the Nimbus Infrared High Resolution Radiometer. Some of these improvements are useful generally, while others are uniquely suited to this application. For example, if a highly sensitive thermistor detector were required for use with a radiometer having a 10 Hz chop frequency, we could make one with a slow response but with a higher detectivity than those constructed for this program. For the present application, which dictates flat response to frequencies of 200 Hz and higher for use in an unchopped system, the series of detectors which we have investigated is certainly much more suitable. In particular, all of the characteristics which we attempted to optimize have yielded some improvements. This section contains a brief discussion of the individual steps taken to optimize the detector characteristics for the Nimbus HRIR application.

## 4.1 Use of Thin Flakes

As is predictable from a theoretical review of the physical properties of the thermistor bolometer, a thinner detector flake can be expected to decrease the detector time constant. Not so easy to predict are effects such as whether this time constant improvement would be accompanied by a degradation in detectivity at low frequencies, whether the noise would be excessive, and whether the detector reproducibility and reliability would be adversely affected. Such side effects are particularly difficult to analyze when dealing with thin films of a substance which may not display the usual bulk properties.

The test results show that the responsivity of the thin detectors, which are one-half the thickness of standard detectors, is about 50% higher than that of standard detectors, as measured at low frequencies at $0.6 V_{pk}$ bias. Since the resistance of these detectors is twice that of the standard thickness flakes, an increase in noise by a factor equal to the square root of the resistance increase (1.41 times) would be expected. This, on the average, is what we have measured. The character of this noise, such as the 1/f characteristic and the knee of the 1/f region, shows no apparent change. We therefore realize a slight net gain in detectivity at low frequencies, plus a very marked decrease in time constant and a consequent significant increase in detectivity at higher frequencies.

## 4.2 Value of Optimizing Blackening

Since operation in the 10 - 12 micron region of the spectrum is intended, we investigated the possibility of using an unblackened or a moderately

blackened thermistor flake, and of determining the trade-offs between possible reduction in absorptance at 10µ and the decreased time constant which results when the blackening agent is used either very sparingly or omitted altogether.

Several additional detectors were fabricated; some were finished with no blackening applied and several with only one coat of black added. The spectral response measurements indicated that the thin flakes had poorer absorptivity, particularly at the shorter wavelengths. At the longer wavelengths, both thin and standard thickness detectors absorbed well even without blackening. At 15 microns, for any system operating in the carbon dioxide band at that wavelength, a totally unblackened flake had a responsivity nearly equal to that of a flake to which the full course of black was applied. Of course, the time constant of such an unblackened flake is much better, as shown in Figures I-1-1 and I-1-2.

In the region of 10 - 12 microns, there is still a difference in responsivity between the blackened and unblackened flake and some blackening is indicated particularly for the thin detectors. However, where a fast time constant is as desirable as in the present application, it seemed practical to examine detectors with only a modest amount of blackening added. This was done with a number of detectors. Totally unblackened thin flake detectors showed a lowered responsivity. However, thin flake detectors with a single coat of APB had responsivities comparable to the more standard test detectors. The time constants of these lightly blackened detectors were about 15% shorter than those of comparable detectors with three coats of the same blackening. These findings made the exercise well worth the effort. The final delivered detector, constructed using this technique, displays a time constant at room temperature and 0.6 $V_{pk}$ of about 800 msec.

## 4.3  Improvement with Detector Cooling

Using the equations given in NAVORD Report No. 5495, the thermal coefficient of resistance of a thermistor increases with a decrease in temperature according to the relationship:

$$\alpha = \frac{dR}{dT}\frac{1}{R} = -\frac{\beta}{T^2} \tag{1}$$

where:

$\alpha$ = thermal coefficient of resistance

T = absolute temperature

$\beta$ = constant associated with detector material

R = resistance

The dependence of noise voltage on temperature is:

$$V_n = (4 \, K \, T \, R \, \Delta f)^{\frac{1}{2}} \qquad (2)$$

where:

$V_n$ = noise voltage

K = Boltzmann constant

$\Delta f$ = bandwidth

The reduced Johnson noise and increased thermal coefficient of resistance, both due to the temperature decrease, result in an improved sensitivity.

Since the detector resistance increases at the lowered temperature, the bias voltage can be increased safely to obtain an increase in responsivity. However, noise voltage also affects responsivity in the following manner:

$$\Re = \left[ V_B \, R \, \epsilon^{\beta/T^2} \right]^{\frac{1}{2}} \qquad (3)$$

Substituting for resistance in Equation 2, $R = \dfrac{V_n^{\,2}}{4 \, K \, T \, \Delta f}$

$$\Re = \left[ V_B \, \frac{V_n^{\,2}}{4 \, K \, T \, \Delta f} \, \epsilon^{\beta/T^2} \right]^{\frac{1}{2}}$$

- 22 -

Thus, the responsivity increase due to increased bias is offset by the higher value of resistance noise. Therefore, the net improvement in detectivity is due mainly to the increased temperature coefficient of resistance (Equation 1) and the slight noise reduction (Equation 2). An improvement in detectivity by a factor of about 1.5 times in the mid-frequency region of operation is achievable with the average detector cooled from +25°C to -25°C. Over a fairly wide range of temperatures, the improvement can be characterized as a detectivity increase of 1% per degree C.

## 4.4 Time Constant Decrease of Cooled Detector

A second effect of cooling the thermistor bolometer is the decreased time constant, a characteristic of both standard thickness and thin flake types. Over a range of about 50°C, the improvement in detector time constant is by a factor of about $\frac{1}{2}$% per °C of ambient temperature decrease.

## 4.5 Biasing of the Detector at Levels Above 0.6 $V_{pk}$

Although the slope of the voltage-current characteristic of a thermistor begins to decline beyond 60% of peak bias (due to increased self-heating), there is a continued increase in responsivity beyond this level. To establish the value of increased bias, we made careful measurements to determine the amount of increase in noise resulting from the increased current before assessing the effect more bias would have on the thermistor's detectivity.

The measurements show some gain in signal-to-noise ratio at 0.8 $V_{pk}$ relative to the 0.6 level, although as was expected, not directly with the bias increase. The 0.9 $V_{pk}$ level showed essentially no further improvement and is not recommended because of the increased danger of thermal runaway. An interesting by-product of the measurement of detector characteristics at the higher bias levels is the discovery of a faster response time in the particular detector configuration and circuit used. An analysis of this time constant improvement with increased bias has been attempted but is not certain to be rigorous and correct. It is therefore not presented in this report. More work along these lines is indicated to obtain a complete understanding of the phenomenon. Our best guess at present is that the time constant improvement for the balanced bridge detector configuration, which characteristically amounts to about 0.5% time constant reduction per 1% bias increase at 25°C and more at lower temperatures, is due to a regenerative feedback effect.

## 4.6 Preamplifier Improvements

The preamplifier for the present application must meet a number of difficult requirements. The instrument must have a high input impedance to accommodate the high source resistance of thin, cooled thermistor bolometers, as well as good response at sub-audio frequencies. It must also have a low noise figure for the high impedance source when operating over the entire frequency range of interest, from 0.05 Hz to about 300 Hz. The importance of a low noise contribution by the preamplifier increases if the instrument is used to make accurate measurements of noise at very low frequencies.

These difficult conditions are best met, in our judgement, by a parametric amplifier such as the SP2A which shows almost no measurable 1/f noise characteristic down to frequencies of 0.01 Hz when used in conjunction with a source impedance of several hundred thousand ohms. The reasoning which led to this choice of a suitable preamplifier is explained in an internal Engineering Memorandum, Appendix A, Part II. This memorandum includes data on noise performance, particularly at low frequencies, of a variety of solid state devices. Figure A1 of that memorandum summarizes the frequency and impedance range over which satisfactory operation can be obtained with various types of preamplifiers.

## 4.7 Importance of Fast Detector Response

To assess the significance of the detector time constant in the application for the Nimbus High Resolution Radiometer and to permit a judicious choice of parameters to yield the optimum system performance, an examination was made of the signal-to-noise ratio to be expected for a given detector time constant.

The system specifications call for a flat signal response extending from about 0.05 Hz to 300 Hz. If the detector had a frequency response with a break-point at 300 Hz, we would have to do no more than to roll off frequencies above this value to reduce the system's high frequency noise.

If the detector were too slow it would have been necessary to boost the high frequencies by providing a lead network with a break-point equivalent to the detector's lag characteristic. We can assume that a dual lag network will be used to begin the high frequency roll-off (3 db point) at 300 Hz.

The Bode characteristic of the amplifier will be as shown in Figure I-4-1.

The transfer function of the amplifier becomes:

$$\frac{e_o}{e_i} = \frac{A(s + \omega_1)}{(s + \omega_2)^2}$$

where:

$e_o$ = output voltage

$e_i$ = input voltage (signal into the equivalent network)

$A$ = gain of amplifier

$s$ = $\sigma + i\omega$; complex variable used in LaPlace transforms*

$\omega_1$ = angular rate corresponding to detector roll-off = $1/\tau_d$

and

$\omega_2$ = cut-off frequency

Insofar as the signal and responsivity are concerned, we can determine from the detector data what the trade-offs are in responsivity when we emphasize speed of response or manipulate various detector parameters.

From the standpoint of noise, the increased gain at higher frequencies and the extension of the response in the high frequency domain which this entails result in increased system noise for the boosted condition.

The noise power can be expressed as:

$$P_n = \int_{-\infty}^{+\infty} A\,G\,(\omega)^2\,d\omega$$

where:

$$G(\omega) = \frac{s + \omega_1}{(s + \omega_2)^2}$$

This expression for noise power can be solved with LaPlace transforms or with a formula such as is given in the Radiation Laboratory Series on Servo Mechanisms**. There we obtain:

$$I_2 = \frac{1 + \omega_1{}^2/\omega_2{}^2}{2 \times 2\,\omega_2}$$

---

*     Korn and Korn, Mathematical Handbook for Scientists and Engineers, McGraw-Hill 1961, p. 8.8-1.

**    James-Nichols-Phillips, Theory of Servo Mechanisms, Vol. 25, Radiation Laboratory Series, McGraw Hill, 1947, p. 369

A normalized form of this expression is plotted for our particular application in Figure I-4-2. The ordinate represents a penalty factor for use of detectors with inadequate response time.

The resulting degradation is a fairly large one in comparison with the increase in responsivity normally associated with thermistors (i.e., Resp. $\sim \sqrt{T_d}$), which is generally a function of the detector substrate chosen and sometimes the amount of blackening applied. As shown with thin flakes, there is no loss in sensitivity at lower frequencies and the time constant improvement is obtained gratis, so to speak.

## 4.8 Detectivity of Cooled Bolometer

It is shown in NAVORD 5495, Appendix C, that in certain cases the NEP of a thermistor bolometer bears the following relationship to operating temperature:

$$NEP = \frac{C \, T_o^{5/2} \, R_o^{\frac{1}{2}}}{V_B}$$

where:

$$V_B = \frac{R_o \, \Delta T^{\frac{1}{2}}}{3 \, Z}$$

and

$R_o$ = flake resistance with zero bias

$\Delta T$ = $T_f - T_o$ = temperature rise of flake ($T_f$) above sink ($T_o$) for bias voltage $V_B$

$Z$ = thermal impedance of barrier between flake and sink (°C/watt)

$C$ = constant

The validity of this equation for the thermistor bolometers fabricated in the present program is borne out by the evaluation of our measurements as embodied in Table I-1-1. There it is apparent that $1/D^*$ does follow a 5/2 power temperature law.
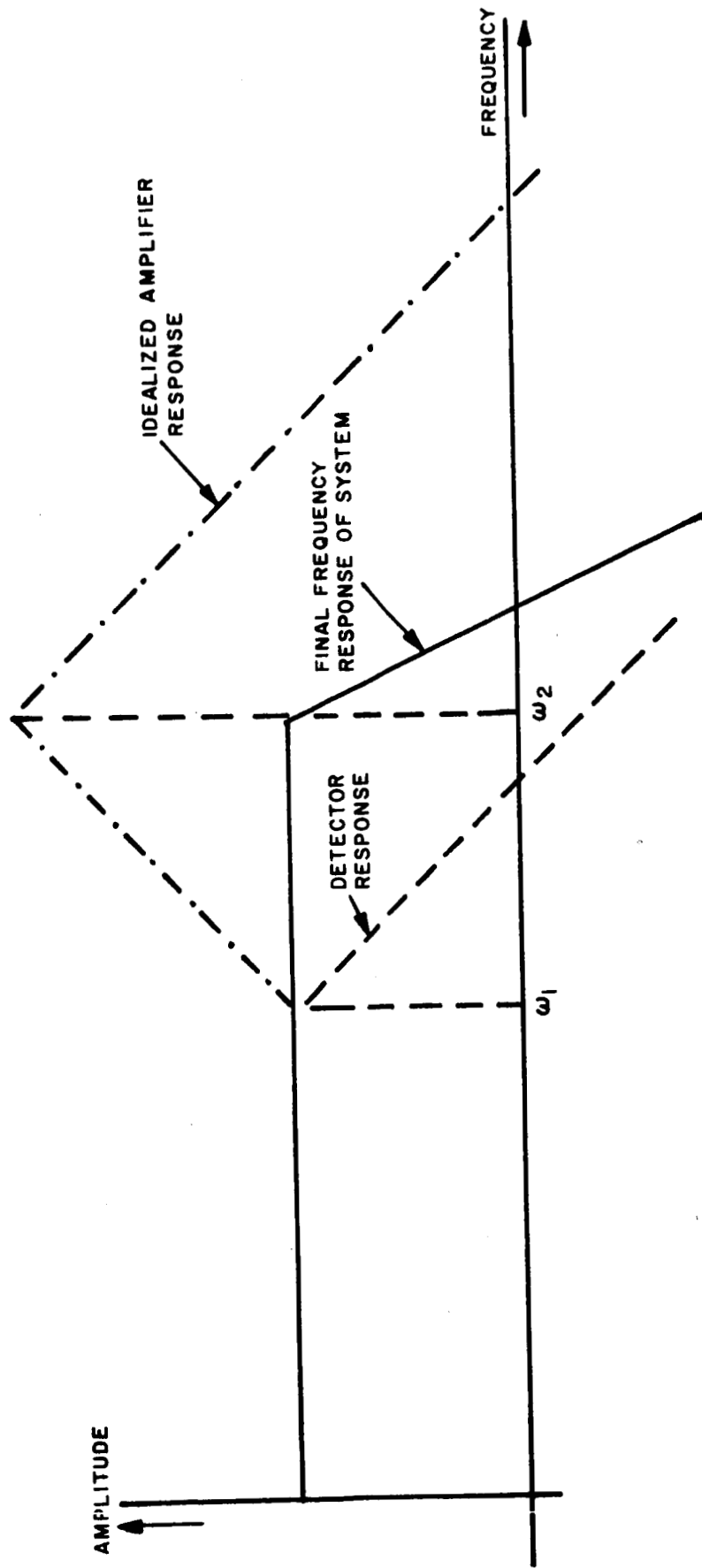
Figure I-4-1  BODE CHARACTERISTIC OF DETECTOR/PREAMPLIFIER COMBINATION
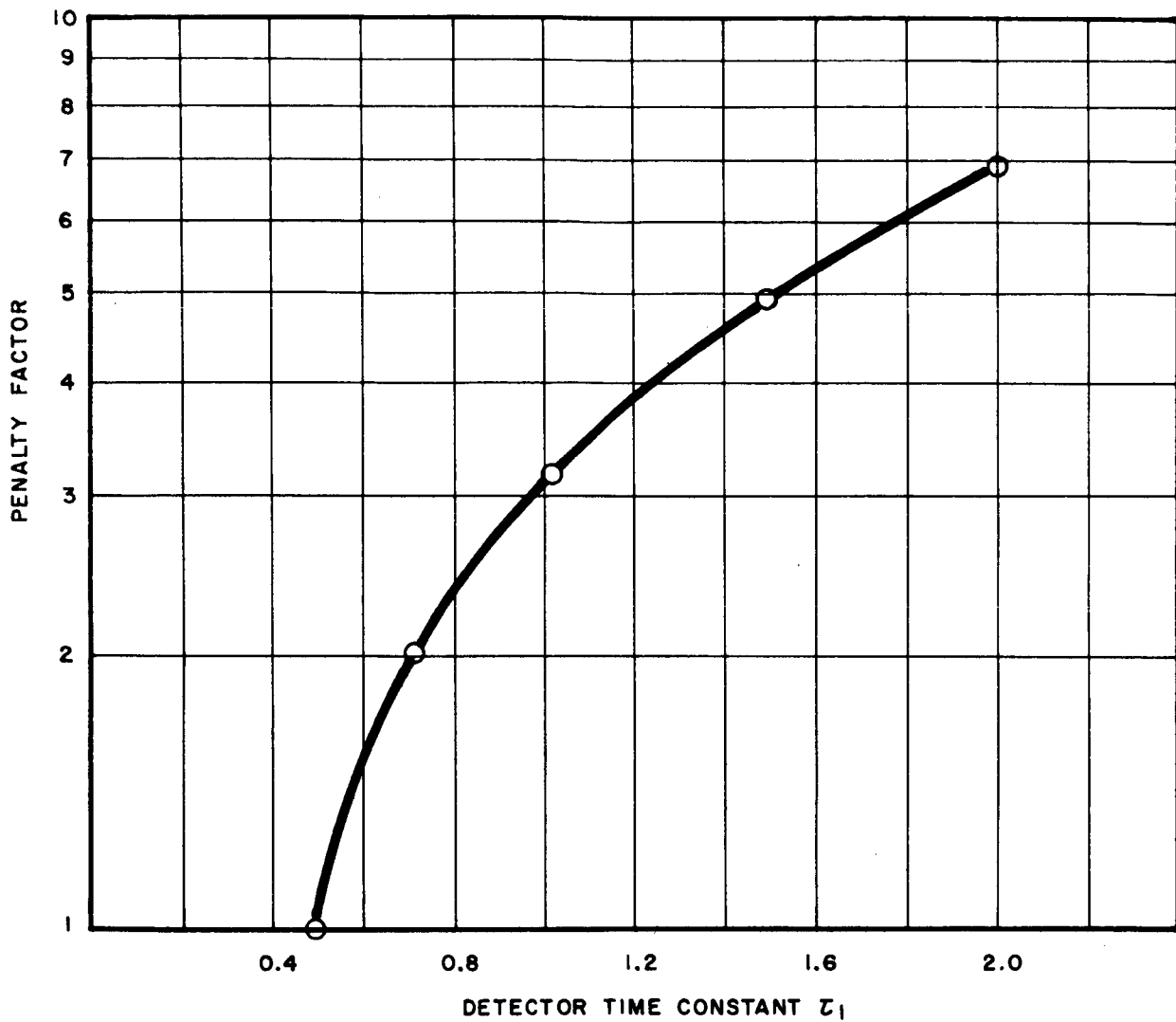
PENALTY FACTOR IS $\dfrac{V_n \text{(BOOST)}}{V_n \text{(NO BOOST}}$
$\qquad\qquad\qquad$ .5 MSEC DET)

WHERE $V_n{}^2 = \displaystyle\int_{\omega_1}^{\omega_2} K \frac{1+\omega_1^{\,2}\tau_1^{\,2}}{(1+\omega_2^{\,2}\,\tau_2^{\,2})^2}\, d\omega$

$\tau_1$ = DET TIME CONST. FOR THE CASE OF
A SYSTEM REQUIRING FLAT RESPONSE
TO 300 Hz; $\tau_2$ = .5 MSEC

Figure I-4-2 PENALTY FACTOR

# 5. OVER-ALL CONCLUSIONS AND RECOMMENDATIONS

The various experiments in detector manufacture and operating parameter determination and the many measurements made as part of this program have provided some improvements in detector performance, and have given us a better understanding of thermistor properties and capabilities. Under the conditions specified, at ambient temperatures between 0° and -25°C and at bias levels of about 0.8 $V_{pk}$ at the operating temperature, the thin (8 micron) germanium-immersed bolometer with a light coat of APB blackening provides a fast time constant averaging around 700μsec. This bolometer also shows a detectivity in the 10 - 12 micron band approaching the thermal noise limit for such a configuration. However, the achievement of this performance also demands a preamplifier with negligible noise contribution and a bias supply which also does not degrade the detector performance. A review of preamplifier performance characteristics has led to the choice of a solid-state parametric amplifier which meets the stringent requirements of our application.

The detector optimization program has also produced some interesting new information, including data and methods for measurement of the 1/f noise characteristics of detectors down to frequencies as low as 0.04 Hz.

In evaluating the results of our various experiments, we have been guided principally by the Nimbus HRIR requirements. These dictate a strong emphasis on fast detector response. We have analyzed the penalty incurred when a slow detector is used, and a consequent high frequency boost is required to provide the desired response to small targets. The large degradation in signal-to-noise ratio (shown in Figure I-4-1) when boosting is required shows the desirability of using a faster detector even at the cost of some loss in responsivity.

In view of the complex character and frequency dependence of thermistor detectivity (see Figure I-1-2) and its effect on over-all picture quality in a thermal imaging system, we believe that the best way to characterize the improvements achieved under our development program is through use of separate figures of merit in the various frequency domains as done in Table I-1-1. However it is possible to evaluate the various measures we have taken to optimize the thermistor detector's performance, basing the evaluation on measurements made on a wideband system - e.g., 0.04 to 300 Hz - with a flat frequency response between these points. We can then assess the significance of the improvements which have been made. Table I-1-2 shows the results of an evaluation of the improvements in signal-to-noise ratio based on the wide-band video signal expected in the Nimbus HRIR scanner.

The most striking measured improvements are in the area of time constant decrease. We have shown (Section 1) that, operating in the 10 - 12 micron region, we approach the thermal noise limit in the mid-frequency range of operation. In addition, the region of high detectivity has been extended to the higher frequencies by about one octave. The possibility of further improvements in the mid-frequency region of operation is rather limited. Areas with considerable room for improvements are the high and low frequency regions of the spectrum. A recently prepared proposal, P-1090A, dated January 10th of this year, recommends a number of measures and outlines a program of investigation to complement the present work, and should lead to improvements principally in the low and high frequency detectivity of thermistors.

The importance of a reduction in 1/f noise in thermistor detectors can be best illustrated with a pictorial example. Figure I-5-1 is a thermograph of a hand and two calibrated test plates. The latter serve as guides in determining contrast levels and sensitivity of the instrument used in producing the thermograph. The immersed thermistor detector used was one quite similar to the type required for the HRIR. The scanner covered one line in 1/4 second with 100 resolution elements for each line (0.1° resolution for a 10° scan). The frequency response used to produce this thermograph was 0.05 Hz to 250 Hz (the 3 db points), and included a modest amount of high frequency boost to provide the desired flat response. Some degradation in sensitivity has resulted from the boosted gain at high frequencies, which increased noise more than signal.

The more serious problem illustrated by this thermograph is the presence of 1/f noise. Because this noise contains long-period positive and negative pulses, it appears as a brightening or darkening of portions of the picture encompassing complete lines or large section of some lines. This type of noise may be more bothersome than the peppery (snow) type characteristic of high frequency white noise. The occurrence of occasional dark or light lines or line segments tends to destroy the radiometric fidelity of a thermal picture. For this reason, we feel a need for more effort in the direction of reducing the prevalence of 1/f noise in thermistor detectors.

We believe that the use of thermistors in the HRIR will add significantly to the quality and value of this important meteorological experiment, providing daylight operation capability and an increase in sensitivity far greater than that achievable with the photoconductive detector. The improvements in detectivity and time response of immersed thermistor detectors, which this study shows to be achievable, add an increased margin of sensitivity which may be used to produce better thermal images or may be employed in a different form to increase the optical or spectral resolution of the Nimbus HRIR system.
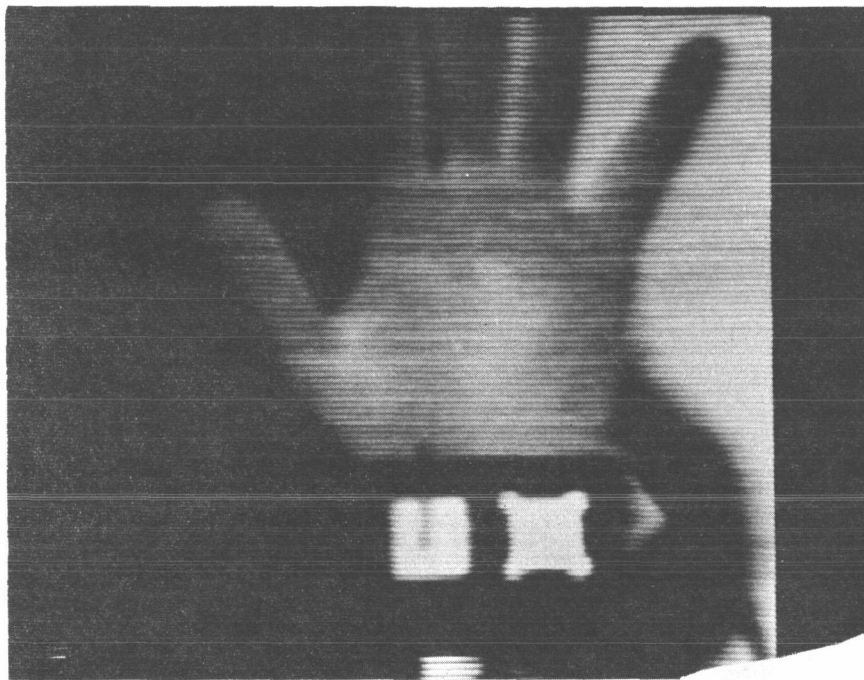
Thermograph of a hand and calibration source. A 0.1mm x 0.1mm
Germanium immersed thermistor was used in a scanning system with
electronics having a frequency response of .05 to 250 Hz. The
black to white contrast is equivalent to $10^{\circ}$C. The target at
right is at a temperature of $39^{\circ}$C and that at the left is $38^{\circ}$C.
Resolution is $0.1^{\circ}$. The system just resolves a vertical black
strip across the target at the left, the strip being about 1/10"
in width. Target distance is 46" and picture scanned is $10^{\circ}$ x $10^{\circ}$.
Note occasional dark and light lines which show evidence of
1/f noise.

Figure I-5-1